Loss of purine salvage in Lesch-Nyhan disease impairs energy metabolism, prevents mTORC1 activation, and reduces developmental potential in midbrain dopaminergic cells

Vincent McCarty

Department of Human Genetics

McGill University, Montréal

August 2021

A thesis submitted to McGill University in partial fulfillment of the requirements of the degree of Master of Science (MSc) in Human Genetics

Dedication

To my mother, Evelyn, who exposed me to the power of science as a means to heal, and to my father, Eric, who has always encouraged me to ask questions and find answers.

"When we try to pick out anything by itself, we find it hitched to everything else in the Universe."

John Muir

Abstract

Lesch-Nyhan disease (LND) is a neurodevelopmental disorder caused by mutations in the gene *HPRT1*, which encodes the purine recycling enzyme, HPRT. Impaired purine recycling leads to overproduction of uric acid, resulting in gout and hyperuricemia. Remarkably, while the brains of individuals with LND appear largely normal, they experience severe neurological symptoms including self-injurious behaviour and motor impairment. While not fully understood, these outcomes have been tied to observations that the brains of those with LND show reductions in tyrosine hydroxylase and dopamine, involved in reward and motor functions. This thesis presents findings of investigations performed using stem cell and genetic engineering technologies to model LND in *HPRT1* knockout and patient-derived forebrain and midbrain cell types. We found that loss of HPRT in dopaminergic (DA) neural progenitor cells (NPC) led to reduced intensity of developmental cell-fate markers, loss of purine derivatives, and impaired glycolysis and oxidative phosphorylation. Real-time glucose tracing revealed that DA NPCs lacking HPRT sacrifice ATP production to prioritize *de novo* purine synthesis. Depleted purines in DA NPC resulted in loss of RHEB, impairing activation of mTORC1. Overall, the data indicate that loss of purine salvage has specific effects in the dopaminergic cell lineage, possibly due to a pre-programmed, higher-energy state in those cells.

Résumé

La maladie de Lesch-Nyhan est un trouble du développement neurologique causé par des mutations du gène *HPRT1*, encodant l'enzyme de recyclage des purines, HPRT. L'altération du recyclage des purines entraîne une surproduction d'acide urique, entraînant la goutte et l'hyperuricémie. Remarquablement, alors que les cerveaux des personnes atteintes de LND semblent en grande partie normal, ils présentent de graves symptômes neurologiques, notamment un comportement d'automutilation et une déficience motrice. Pas encore entièrement compris, ces symptômes ont été liés à des observations que les cerveaux des personnes atteintes de LND présentent des réductions de la tyrosine hydroxylase et de la dopamine, impliquées dans les fonctions de la récompense et motrices. Cette thèse présente les résultats d'enquêtes réalisées à l'aide de technologies de cellules souches et de génie génétique pour modéliser le LND dans les cellules knock-out *HPRT1* ou dérivées des patients, de types du cerveau antérieur et du cerveau moyen. Nous avons constaté que la perte de HPRT dans les cellules progénitrices neurales dopaminergiques (DA NPC) entraînait une réduction de l'intensité des marqueurs du destin cellulaire du développement, une perte de dérivés de purine et une altération de la glycolyse et de la phosphorylation oxydative. Le traçage du glucose en temps réel a révélé que les DA NPCs dépourvu de HPRT sacrifient la production d'ATP pour prioriser la synthèse des purines. La perte de purines dans DA NPC a entraîné la perte de RHEB, altérant l'activation de mTORC1. Dans l'ensemble, les données indiquent que la perte de recyclage des purines a des effets spécifiques dans la lignée cellulaire dopaminergique, probablement en raison d'un état d'énergie plus élevée préprogrammé dans ces cellules.

Table of Contents

List of Abbreviations

13C	carbon-13
2-DG	2-deoxy-D-glucose
ADHD	attention deficit hyperactivity disorder
ADP	adenosine diphosphate
AICAR	5-aminoimidazole-4-carboxamide-1-β-D-ribofuranoside
AMP	adenosine monophosphate
AMPK	AMP-activated kinase
ARL13B	ADP-ribosylation factor-like protein 13B
ASD	autism spectrum disorder
ATP	adenosine triphosphate
BCA	Bicinchoninic acid
BrdUTP	5-Bromo-2'-deoxyuridine-5'-triphosphate
BSA	bovine serum albumen
C13	carbon-13
Cas9	CRISPR associated protein 9
cDNA	complementary DNA
CN	cortical
CRISPR	clustered regularly interspaced short palindromic repeats
DA	dopamine/dopaminergic
DAPI	4′,6-diamidino-2-phenylindole
DBS	deep brain stimulation
DMEM	Dulbecco's Modified Eagle Medium
DNA	Deoxyribonucleic acid
dNTP	Deoxynucleoside triphosphate
DOPAC	3.4-Dihydroxyphenylacetic acid
DSM-V	diagnostic and statistical manual of mental disorders
DTT	Dithiothreitol
ECAR	extracellular acidification rate
FCCP	Carbonyl cyanide-p-trifluoromethoxyphenylhydrazone
FOXA	Forkhead Box A
G6P	glucose-6-phosphate
GDP	guanosine diphosphate
GLI	Glioma-Associated Oncogene Family Zinc Finger
GMP	guanosine monophosphate
GTP	guanosine triphosphate
HPLC	high performance liquid chromatography
HPRT	hypoxanthine-guanine phosphoribosyl transferase
HVA	homovanilic acid

ICC	immunocytochemistry
IFT88	Intraflagellar Transport 88
IMP	inosine monophosphate
iPSC	induced pluripotent stem cell
KCL	Potassium chloride
KLF4	Kruppel Like Factor
KO	knockout
LMX1A	LIM Homeobox Transcription Factor 1 Alpha
LND	Lesch-Nyhan disease
LNV	Lesch-Nyhan variant
mRNA	messenger ribonucleic acid
MTORC1	mammalian target of rapamycin complex 1
NPC	neural progenitor cell
Nurr1 / NR4A2	nuclear receptor 4A2
OCR	oxygen consumption rate
OCT	octamer-binding transcription factor
OXPHOS	oxidative phosphorylation
PBS	Phosphate-buffered saline
PET	positron-emission tomography
PPP	pentose phosphate pathway
PRPP	5-phosphoribosyl 1-pyrophosphate
qPCR	quantitative polymerase chain reaction
R5P	ribose-5-phosphate
RHEB	Ras homolog enriched in brain
RNA	ribonucleic acid
RT	reverse transcriptase
Ser	Serine
SHH	sonic hedgehog
ShRNA	short hairpin ribonucleic acid
SOX	sex determining region Y-box
TDH	L-threonine dehydrogenase
TH	tyrosine hydroxylase
Thr	Threonine
TOMM20	Translocase Of Outer Mitochondrial Membrane 20
TSC	Tuberous sclerosis complex
TUNEL	Terminal deoxynucleotidyl transferase dUTP nick end labeling
ULK1	Unc-51 Like Autophagy Activating Kinase 1
VTA	ventral tegmental area

List of Figures

Thesis Figures:

Manuscript Figures:

Acknowledgements

I would like to acknowledge:

Dr. Carl Ernst, for his supervision and guidance. Carl's optimistic, calm, and compassionate approach to leadership and life is something I can only hope to emulate in my own undertakings.

Dr. Scott Bell, who mentored me in the lab before graduating with his PhD. Though he officially trained me in laboratory techniques, I learned far more from Scott through many hours of conversation and gained a friend in the process.

Dr. Huashan Peng, Dr. Xin Zhang, and Ying Zhang, members of the Ernst lab whose hard-work, knowledge, and technical excellence in the Ernst lab made my research possible.

My fellow students in the Ernst lab, Malvin Jefri, Nuwan Hettige, Lilit Antonyan, Anjie Ni, and Shaima Alsuwaidi, whose help, advice, and company in the lab enriched my experience.

The Department of Human Genetics at McGill University, namely Ross Mackay and Rimi Joshi, whose consistent and prompt counsel helped me navigate the path to completion.

Dr. Loydie Majewska, Dr. Jo Anne Stratton, Dr. Pierre Moffatt, and Dr. Yojiro Yamanaka, professors at McGill University who generously offered their time to make my supervisory meetings, seminar, and thesis submission possible.

Co-authors on the included manuscript, for contributing to my research and for participating in the important endeavor that is science.

My parents, Evelyn and Eric, my sisters, Karina and Briana, and my Oma, Berta, for their permanent presence and support in my life.

My friends, including my fellow academic, Phil, who was by my side in CEGEP and for five years of university.

My partner, Benjamin, for being on this journey with me.

Format of Thesis

This thesis is presented in a manuscript-based format, expanding on: “Lesch-Nyhan disease causes impaired energy metabolism and reduced developmental potential in midbrain dopaminergic cells” published in Stem Cell Reports in July 2021. With the permission of co-first author Scott Bell, PhD, the content of the article is reproduced herein as Chapter 3 exactly as published.

Contribution of Authors

Chapter 1: Introduction and **Chapter 2: Methods**

Written by Vincent McCarty

Chapter 3: Manuscript in Stem Cell Reports

Scott Bell[#], Vincent McCarty[#], Huashan Peng, Malvin Jefri, Nuwan Hettige, Lilit Antonyan, Liam Crapper, Liam A. O'Leary, Xin Zhang, Ying Zhang, Hanrong Wu, Diane Sutcliffe, Ilaria Kolobova, Thad A. Rosenberger, Luc Moquin, Alain Gratton, Jelena Popic, Ilse Gantois, Patrick S. Stumpf, Andreas A. Schuppert, Naguib Mechawar, Nahum Sonenberg, Michel L. Tremblay, Hyder A. Jinnah, and Carl Ernst

#: co-first authors

S.B., V.M., and C.E. wrote the manuscript and were involved in all aspects of the design and execution of the study. H.P., M.J., N.H., L.A., L.C., L.A.O., X.Z., Y.Z., H.W., and I.K. performed experiments. D.S., N.M., and H.A.J. contributed reagents and advised on study design; T.A.R., L.M., and A.G. performed HPLC. J.P., I.G., and N.S. performed and interpreted protein assays related to mTORC1; P.S.S. and A.A.S. performed statistical analyses. M.L.T. coordinated and supervised the Seahorse experiments.

More specifically, I, Vincent McCarty, contributed a significant portion of the laboratory work, including culture of cells used in assays, ICC, western blotting, qPCR, imaging, image analysis, and statistical analysis. I was also a major contributor in the writing of the manuscript and supplemental information, submission, and revision of the manuscript. I also led the design process of all figures.

Chapter 4: General Discussion and **Chapter 5: Conclusions and Future Directions**

Written by Vincent McCarty

Chapter 1: Introduction

Neurodevelopmental Disorders

According to the DSM-V, neurodevelopmental disorders are characterized by impairments of personal, occupational, social, or academic functioning with onset in the developmental period (American Psychiatric Association 2013). This broad categorization means that the group of conditions referred to as neurodevelopmental disorders presents a wide range of symptoms, impairments, severities, and etiologies. Additional diagnostic complexity is introduced by frequent co-occurrence of multiple neurodevelopmental disorders in one individual. Autism spectrum disorder (ASD), for example, is known to regularly co-occur with intellectual developmental disorder (American Psychiatric Association 2013).

A 2017 study of more than 180,000 children between 6 and 10 years of age registered with the British Columbia Medical Services Plan found that 8.3% met criteria for diagnosis with a neurodevelopmental disorder (Arim et al. 2017).

While many common neurodevelopmental disorders such as ASD or attention-deficit hyperactivity disorder (ADHD) are presumed to be multifactorial in their etiology, others are understood to result from a distinct root cause (Bishop 2010). This is the case for fetal alcohol syndrome, as well as the many disorders which arise from various genetic abnormalities, including Fragile X syndrome, Down syndrome, and Rett syndrome(Bishop 2010).

Epidemiology of Lesch-Nyhan disease

Identified in 1964, Lesch-Nyhan disease is among the rarest and most severe forms of neurodevelopmental disorders. A 1972 publication estimated the annual live birth rate of Lesch-Nyhan disease in Canada to be 1 in 380,000 live births (Crawhall, Henderson, and Kelley 1972). In a 2007 interview, Dr. William Nyhan, co-discoverer of the disease, estimated there to be “a few

hundred" individuals living with Lesch-Nyhan disease in the United States population of approximately 300 million (Preston 2007).

HPRT1, the gene encoding Hypoxanthine-guanine phosphoribosyltransferase

In 1967, Lesch-Nyhan disease was found to be caused by mutations in the gene *HPRT1*, which encodes Hypoxanthine-guanine phosphoribosyltransferase, also known as HPRT or sometimes HGPRT, a key enzyme for recycling purines in the cell (Seegmiller, Rosenbloom, and Kelley 1967).

While Lesch-Nyhan disease is rare, the gene responsible is among the most commonly known in the genome. This is because *HPRT1* is often used as a "housekeeping" gene, used to normalize measurements of expression in assays such as quantitative polymerase chain reaction (qPCR) because it is thought to maintain a relatively high and stable level of expression(Silver et al. 2006). The homolog of *HPRT1* in the mouse genome, known as *Hprt*, was the first endogenous gene to undergo targeted mutagenesis or be "knocked-out". Published in 1987, this research was later recognized with the 2007 Nobel Prize for Physiology or Medicine(Thomas and Capecchi 1987; Kuehn et al. 1987).

HPRT1 is approximately forty-five thousand base pairs long, comprised of nine exons and eight introns, and is found on the X chromosome near position Xq26.1(Nguyen, Naviaux, and Nyhan 2017; Jinnah et al. 2000). As a result of the position of *HPRT1* in the genome, Lesch-Nyhan disease follows an X-linked recessive inheritance pattern and affects almost exclusively males. Cases of Lesch-Nyhan disease can rarely occur in females when non-random X inactivation prevents *HPRT1* expression from the healthy X chromosome(Jinnah et al. 2000). As of 2017, more than 600 mutations in *HPRT1* had been identified in patients with Lesch-Nyhan disease, including insertions, deletions, and mutations involving single base pairs, which are most common (Nguyen,

Naviaux, and Nyhan 2017). These single base substitutions account for 63% of cases and include missense, nonsense, and splicing error mutations (Jinnah et al. 2000).

Data from the year 2000 indicated that while some regions of the gene tend to be mutated more often than others, most mutations that affected substrate binding occurred outside the region encoding the substrate binding domain identified by X-ray crystallography(Jinnah et al. 2000). Though one could hypothesize that the HPRT protein may have yet-undiscovered function. This more likely suggests that the functional activity of HPRT's active site is vulnerable to indirect conformational change, meaning mutations distant from the binding domain may cause a change in conformation of the HPRT protein more generally which in turn affects the conformation of the active site and prevents the active site from functioning appropriately.

Simultaneously, different mutations in *HPRT1* can impair the enzyme activity of HPRT to varying degrees (Sampat et al. 2011). When an individual's HPRT enzyme activity is approximately 1.5% or less, they experience the most severe phenotype of *HPRT1* mutation: Lesch-Nyhan disease (Sampat et al. 2011). When enzyme activity is above this threshold, the condition is referred to as Lesch-Nyhan variant or Kelley-Seegmiller syndrome (Rosa J. Torres and Puig 2007). Patients with this condition still experience symptoms associated with high levels of uric acid in the body. They may also have neurological symptoms associated with motor function when enzyme activity is below 8%, but do not exhibit self-injurious behaviour (Sampat et al. 2011).

Hypoxanthine-guanine phosphoribosyltransferase (HPRT)

HPRT exists as a tetramer in solution to perform its enzymatic function. Each monomer is composed of 218 amino acids and makes contact with its counterparts via three distinct interfaces (Nguyen, Naviaux, and Nyhan 2017). While the relationship between mutation position and

phenotype severity in Lesch-Nyhan disease is not yet fully understood, these interfaces are likely integral to the enzyme's stability and activity(Nguyen, Naviaux, and Nyhan 2017).

In the cell, HPRT catalyzes the synthesis of the nucleotides inosine monophosphate (IMP) and guanosine monophosphate (GMP) by recycling the purine bases hypoxanthine and guanine, respectively. To do this, HPRT catalyses the transfer of a 5-phosphoribosyl group from the co-substrate 5-phosphoribosyl 1-pyrophosphate (PRPP)(Rosa J. Torres and Puig 2007). When HPRT activity is impaired, the purine bases hypoxanthine and guanine cannot be recycled and therefore accumulate. This accumulation is addressed in the cell by the enzyme xanthine oxidase, which converts them into xanthine and subsequently the toxic waste product uric acid (Rosa J. Torres and Puig 2007). Deficiency in HPRT also causes reduced purine salvage output of IMP, which can be converted to adenosine monophosphate (AMP), and GMP. These molecules and their derivatives play many important roles in the cell, including intracellular signalling, DNA and RNA synthesis, and energy transfer and storage (Zaccolo 2011).

De novo purine synthesis

To compensate for less synthesis of IMP and GMP when purine salvage is impaired, the cell can respond by upregulating the synthesis of these molecules via a process known as *de novo* purine synthesis. The pathway begins with the input of one molecule of PRPP, a product of the pentose phosphate pathway which is derived from glucose-6-phosphate (G6P). This method of producing IMP and GMP from PRPP involves six different enzymes across ten steps and is far less resource efficient than purine salvage(Yin et al. 2018).

Starting with PRPP, the synthesis of one IMP molecule via the *de novo* purine synthesis requires five molecules of ATP, two glutamine, two 10-formyltetrahydrofolate, one glycine, one aspartate, and one carbon dioxide (Yin et al. 2018). To produce GMP or AMP, this IMP molecule

must undergo two more enzymatic transformations, each requiring additional resources which differ depending on the end product(Yin et al. 2018).

Clinical presentation of Lesch-Nyhan disease

Without functional HPRT, impaired purine recycling leads to increased formation of uric acid. Formed as a waste product, uric acid in elevated levels (hyperuricemia when measured in the blood) can result in crystal formation, leading to tissue damage and pain throughout the body (Jinnah et al. 2006). The first sign of Lesch-Nyhan disease is often observed in the baby's diaper, in the form of orange uric acid crystals excreted in the urine. When formed in the soft tissue of the joints, crystals can assemble into tophi and lead to gout and joint damage. In the kidneys, high levels of uric acid can produce kidney stones (nephrolithiasis) which can damage the kidneys and eventually result in renal failure (Jinnah et al. 2006).

The first sign of neurological impairment in individuals with Lesch-Nyhan disease is delayed development of motor skills, which is typically detected between three and six months of age(Jinnah et al. 2006). A variety of motor symptoms have been observed in individuals with Lesch-Nyhan disease, with patients commonly exhibiting a lack of muscle tone (hypotonia) and a lack of motor control (dystonia). Other motor symptoms often seen in cases of Lesch-Nyhan disease include choreoathetosis, opisthotonos, hypertonia, spasticity, hyperreflexia, and dysarthria (Jinnah et al. 2006). As a result of these symptoms, people with Lesch-Nyhan disease cannot walk, require support to sit up, and have impaired speech (Nyhan 1997).

Perhaps the most remarkable and unfortunate characteristic of Lesch-Nyhan disease is compulsive self-injurious behavior, which is observed in nearly all individuals with the disease. Self-injury is usually first seen as biting of the lips or fingers (Nyhan 1997). First onset of self-injury typically occurs between 1 and 10 years of age, with earlier onset being predictive of the

severity of the self-injurious behaviour later on (Anderson and Ernst 1994). The behaviour, often triggered by stress, can result in serious tissue damage, with patients commonly losing tissue around the lip or even partially amputating fingers. Removal of the teeth by a dentist is often necessary to prevent further loss of tissue, with 60% of patients in a 1994 study having undergone dental extraction (Nyhan 1997; Anderson and Ernst 1994).

While there are other conditions which feature self-injurious behaviours, Lesch-Nyhan disease is notable for the variety of injurious behaviours exhibited and for the fact that patients do feel pain and regret their actions. According to Dr Nyhan, the patients are "only limited by the imagination and by the nature of the motor defect" when self-injuring and both feel and fear the pain they inflict upon themselves (Nyhan 1997). In addition to biting their lips, fingers, arms, tongue, and shoulders, people with Lesch-Nyhan disease commonly self-injure by banging their heads, poking their eyes, or touching hot objects.

Though typically followed by remorse, people with Lesch-Nyhan disease may also feel compelled to attempt to injure others (Nyhan 1997). In a 1994 study of 40 patients with Lesch-Nyhan disease, 35 (87.5%) were reported to be aggressive toward others(Anderson and Ernst 1994).

Because of their disordered behaviour and movement, people with Lesch-Nyhan disease are usually found in wheelchairs. To prevent self-injury, protective wraps or gloves are commonly worn on the hands (Nyhan 1997). The 1994 study found that approximately 78% of patients were restrained 50% of the time or more. Perhaps unexpectedly, patients commonly participated in decisions regarding timing and type of restraints, with approximately 92% liking to be restrained and feeling "at ease" (Anderson and Ernst 1994).

Management of Lesch-Nyhan disease

In addition to using a wheelchair, protective equipment, restraints, dental extraction and avoiding stressful triggers to lessen the consequences of self-injurious behaviour, managing Lesch-Nyhan disease involves the use of pharmaceutical interventions. A study of 44 cases of Lesch-Nyhan disease found that, with the exception of one, all individuals were receiving allopurinol to address the overproduction of uric acid (Jinnah et al. 2006). Allopurinol, a structural analogue of hypoxanthine and xanthine, works by competitively binding the enzyme xanthine oxidase, preventing the enzyme from converting xanthine to uric acid (Murrell and Rapeport 2012). Though it does not modify neurological symptoms, this treatment has proven very effective at reducing the serum concentration of uric acid by 50% on average in patients with Lesch-Nyhan disease. It is worth noting that while uric acid levels are reduced, allopurinol drives an increase in levels of xanthine, which can also form stones (xanthine lithiasis), albeit with a lesser frequency. Other methods of addressing symptoms associated with uric acid including hydration and urine alkalinization (R. J. Torres, Prior, and Puig 2006).

Unlike elevated uric acid, the neurological symptoms of Lesch-Nyhan disease have proven much difficult to address. Patients have been prescribed a variety of medications including muscle relaxants, benzodiazepines, and dopamine receptor antagonists in attempt to treat motor symptoms, but none have shown clear improvement (Jinnah et al. 2006).

Interestingly, a recent analysis of long-term outcomes from the perspectives of 14 patients with Lesch-Nyhan disease found that deep brain stimulation (DBS) of the globus pallidus may be worthwhile for the treatment of both motor and behavioural symptoms (Visser et al. 2021). Prior small studies have shown that DBS was associated with a reduction of self-injurious behaviour and the severity of dystonia (Taira, Kobayashi, and Hori 2003; Deon et al. 2011). While many

families in the study offered a positive assessment of DBS, only approximately half of the families would repeat the procedure. This is because 13 of the 14 patients experienced adverse events following the surgery to insert the electrodes required for DBS. These adverse events, mostly post-operative infections and malfunctioning hardware, lead to 12 of the patients undergoing one or more additional surgical procedures (Visser et al. 2021). The findings suggest that improvements in technique and technology may unlock DBS as a worthwhile treatment for the difficult neurological symptoms of Lesch-Nyhan disease.

Neurobiological findings in Lesch-Nyhan disease

Despite the severe symptoms and consequences of impaired neurodevelopment in patients Lesch-Nyhan disease, their brains show little sign of consistent morphological abnormality. In fact, a detailed histopathological study of the brains of eight deceased patients in 1982 found no abnormalities (Watts et al. 1982).

In contrast to the morphological evidence, biochemical signs of pathology in the brains of patients with Lesch-Nyhan disease are apparent and have been well-documented. A 1981 study of the brains of three individuals with Lesch-Nyhan disease found that nearly all biochemical measures of function in striatal dopamine neuron terminals were reduced between 10% and 30% of control values (KG et al. 1981). Data from positron-emission tomography (PET) using a fluorescently labelled dopamine fluorodopa F18 in 12 patients and 15 controls showed that individuals with Lesch-Nyhan disease had reduced fluorodopa F18 activity in the ventral tegmental complex (57% of control), frontal cortex (44%), caudate nucleus (39%), and putamen (31%)(Ernst et al. 1996).

More recent investigation has further supported these findings. A 2014 post-mortem study of five brains found no consistent degeneration or morphological abnormality in any brain region but

did identify a significant reduction in the expression of tyrosine hydroxylase (TH) in the striatum. Though there was a reduction in TH, which is a key enzyme in the synthesis of dopamine, no loss of midbrain dopamine neurons was observed (Göttle et al. 2014).

Taken together, the evidence suggests that the brains of those with Lesch-Nyhan disease contain the neurons which arrange to form dopaminergic pathways, but that despite their undisturbed presence, these cells do not function normally, as indicated by reduced synthesis of dopamine and associated molecules.

In the brain, dopamine neurons assemble to form dopaminergic pathways, including the nigrostriatal, the mesolimbic, and the mesocortical. The nigrostriatal pathway, involved in Parkinson's disease, mainly regulates motor function, originates in the substantia nigra, and projects to the caudate nucleus and putamen in the basal ganglia (Ayano 2016). The mesolimbic pathway, which mediates pleasure, emotion, addiction, and reward, originates in the ventral tegmental area (VTA) and extends to the nucleus accumbens, amygdala, pyriform cortex, and lateral septal nuclei (Ayano 2016). The mesocortial pathway, projecting from the ventral tegmental area to the frontal cortex and septohippocampal regions, is involved in memory, cognition, and emotional behaviour (Ayano 2016).

Energy and Metabolism in the context of Lesch-Nyhan disease research

Inability to salvage purines as a result of HPRT deficiency requires the cell to attempt to compensate with *de novo* purine synthesis, a far less efficient process. Reduction in purines and the consumption of extra resources required to support *de novo* purine synthesis (such as PRPP, ATP, amino acids, and 10-formyltetrahydrofolate) have the potential to disrupt the delicate energetic and metabolic balance required to maintain a healthy cell. Additional 10-formyltetrahydrofolate, for example, must be produced via one-carbon metabolism (Ducker and

Rabinowitz 2017). PRPP is the output of the pentose phosphate pathway, which requires the input of G6P. To source G6P, the pentose phosphate pathway must pull it away from glycolysis, which produces G6P in its first step (Diagram 1). Most of the ATP used in the *de novo* purine synthesis pathway must be produced via oxidative phosphorylation in the mitochondria, a process which, among other resources, requires the end-product of glycolysis, pyruvate.

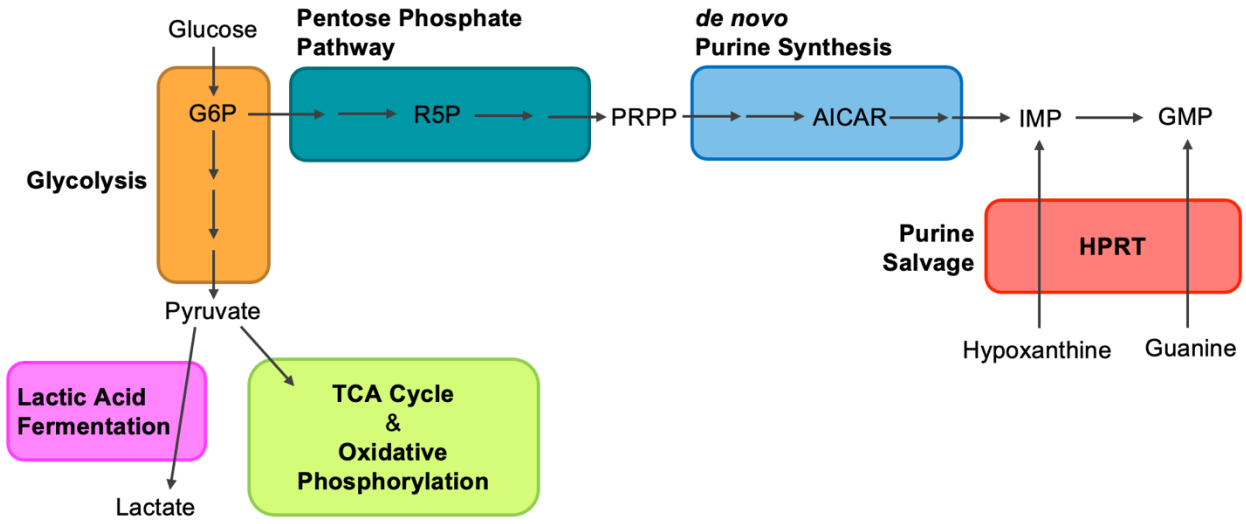

Diagram 1. Simplified schematic of relevant metabolic processes demonstrating the possibility for glucose derivatives to be pulled from energy production to support the synthesis of purines in the event that purine salvage is interrupted.

Glycolysis, oxidative phosphorylation, the pentose phosphate pathway, and the *de novo* purine synthesis pathway represent only a fraction of the entire intricate network of interlinked metabolic pathways and processes that keep a cell alive. To maintain homeostasis, the delicate balance of processes and metabolites must be tightly regulated. Directing this cellular symphony are, among others, AMP-activated kinase (AMPK) and the mammalian target of rapamycin complex 1 (mTORC1).

AMPK is a heterotrimeric complex of proteins which senses the ratio of AMP to ATP in the cell and is activated when bound by AMP. In response to activation, AMPK regulates processes that consume ATP, such as glycoprotein synthesis, and promotes processes which increase ATP, such as glycolysis (Holczer et al. 2019). Similarly, mTORC1 regulates metabolism and cell growth in response to sensed levels of energy, nutrients, and growth factors. To be activated, mTORC1 requires GTP-bound RHEB, whose levels reflect purine concentration in the cell. Among other functions, active mTORC1 phosphorylates signalling proteins including ULK1 and ribosomal protein S6 to inhibit autophagy and drive protein synthesis. Studies have shown that prolonged depletion of purines reduces of levels of RHEB, an obligate activator of mTORC1(Emmanuel et al. 2017; Hoxhaj et al. 2017).

Interestingly, recent findings have also revealed a regulatory relationship between mTORC1 and the primary cilia(Foerster et al. 2017). The primary cilium is an antenna-like organelle involved in signalling processes including the Sonic hedgehog (SHH) pathway. The Shh pathway is vital to normal neurodevelopment and contributes to spatial patterning, cellular identity in the central nervous system, axonal guidance, and the connectivity and activity of neurons (Park, Jang, and Lee 2019). Notable for investigators of Lesch-Nyhan disease, SHH activity is necessary for the differentiation of midbrain dopaminergic neurons (Cooper et al. 2010).

Scientific models for investigating Lesch-Nyhan disease

In addition to direct studies of the brains of patients with Lesch-Nyhan disease via PET imaging or autopsy, models have been used in attempt to understand the neurological underpinnings of the disease. These have included both animal and human cell models.

HPRT1 knockout mice have been found to recapitulate some of the observations seen in individuals with Lesch-Nyhan disease, such as impaired purine recycling and reduction in

dopamine in the brain. They do not, however, reproduce observations such as uric overproduction of uric acid or neurobehavioural abnormality (Jinnah 2009). It is also important to note that human metabolism is not perfectly reflected by mice. The enzyme L-threonine dehydrogenase (TDH), for example, is not functional in humans despite being active in most animals, including mice. In non-humans, TDH is an important provider of the glycine used in one-carbon metabolism for the synthesis of 10-formyltetrahydrofolate, a necessary input for *de novo* purine synthesis (Ducker and Rabinowitz 2017).

Cell lines obtained from human brain tumors have also been used with some success to study Lesch-Nyhan disease, however their genetic and cell type instability have proven suboptimal for generating clear results (Bitler and Howard 1986; Yeh, Zheng, and Howard 1998; Paul et al. 2007; Gao et al. 2016). Ideally, when cell culture is used to study a disease, the cells should be the same cell type as the cells involved in the condition being studied. For example, the neurons of a person with a genetic disease affecting their liver will contain the same affected genome but may not present the pathological phenotype affecting the cells in the liver due to different cell type. In recent years, technological breakthroughs have allowed for the reprogramming of healthy somatic cells to induced pluripotent stem cells (iPSC), from which a vast array of cell types can be differentiated, cultured, and studied (Takahashi et al. 2007). For the purposes of studying neurodevelopmental disorders such as Lesch-Nyhan disease, these can include neural progenitor cells (NPCs) and neurons of various subtypes, including dopaminergic and cortical.

Objectives and Hypothesis

The objective of the following investigations is ultimately to further our understanding of the process by which mutations in *HPRT1*, a gene encoding an enzyme for purine salvage, can lead to a severe and consequential loss of dopamine in the brain.

Specifically, this involves answering the following three questions:

1. *When in neurodevelopment, modelled in vitro, do cells with HPRT deficiency begin to show effects of loss of HPRT and which cell lineages are affected?*
2. *Is there a pre-existing property of those affected cell lineages that caused them to be vulnerable to HPRT deficiency when related neural cell lineages are not affected?*
3. *Concerning the cell lineages which do show effects of HPRT loss, what is occurring in those cells as a result of HPRT deficiency that could explain reduced dopamine in the brain?*

The central hypothesis to this investigation is that the dopaminergic lineage of cells in the developing brain is especially vulnerable to the loss of purine salvage caused by HPRT deficiency and as a result does not yield fully functional dopaminergic neurons, reducing dopamine output.

Chapter 2: Methods

This chapter includes content modified from the supplemental information (Bell et al. 2021).

Cells, cell culture, and genetic engineering (see also: Chapter 3)

The investigations discussed and shown in Chapter 3 were performed using cultured human cells. These cells were received by the lab as fibroblasts which were collected from both healthy donors as well as patients with a range of mutations in the gene *HPRT1*, leading to varying degrees of HPRT deficiency. Further details about cell culture methods can be found on pages 53 and 54 in Chapter 3 of this document as they are included in the main text of the manuscript on which this thesis is based.

Once received, fibroblasts were reprogrammed to become induced pluripotent stem cells (iPSCs) using episomal reprogramming vectors containing Oct4, Sox2, Myc3/4, Klf4, ShRNA P53 (ALSTEM). In the case of genetic engineering of *HPRT1* knockouts using CRISPR-Cas9, it was performed simultaneous to the reprogramming to iPSC. Two *HPRT1* knockout lines, KO1 and KO2, were used in the investigations, with CRISPR-induced deletions in Exon 1 of 23 and 29 base pairs, respectively. iPSCs were assessed for expression of appropriate markers, including SOX2 and OCT4.

Once iPSC lines of control, *HPRT1* knockout, and patient cells were established, they could be expanded, or further induced to become neural progenitor cells (NPCs), which have a distinct morphology from iPSCs. Two types of NPC were produced and investigated in this study: cortical (CN) NPC and dopaminergic (DA) NPC. CN NPCs were assessed for expression of appropriate markers, including SOX1 and PAX6. DA NPCs were assessed for expression of appropriate markers, including Nurr1 and FOXA2. A “crossover” experiment confirmed that CN NPCs and DA NPCs expressed their own markers and did not express each other’s markers. CN NPCs and

DA NPCs were further differentiated to post-mitotic CN and DA neurons, which were confirmed to exclusively express TH and FOXG1, respectively.

Immunocytochemistry (ICC)

Cells cultured on and adhered to cover slips were washed with PBS and fixed with 4% paraformaldehyde (Sigma-Aldrich) on slides for 10 min. 0.1% TX-100/PBS (Sigma-Aldrich) was introduced for 10 min to permeabilize samples before they were blocked in 10% BSA/PBS for 60 min. Primary antibodies were prepared as per manufacturer recommendations in 5% BSA/PBS and added to samples for overnight incubation at 4˚C. Samples were then washed three times in PBS. Secondary antibody diluted according to manufactured recommendations in 5% BSA/PBS was added to the samples before they were incubated for 60 min away from light. Samples were then washed three times with PBS, mounted to slides with VECTASHIELD (Vector Laboratories), and imaged using an AxioImager microscope (Zeiss). Details about the methodology for quantifying the expression levels of stage-specific and cell fate markers in cells which underwent immunocytochemistry and imaging can be found in Chapter 3 on page 55.

Western blot

Cultured cells were lysed with RIPA buffer (Sigma) that had been supplemented with SIGMAFAST Protease Inhibitor Tablets (Millipore-Sigma) and PhosSTOP phosphatase inhibitor tablets (Sigma-Aldrich). Concentrations of protein were measured with a Pierce BCA Protein Assay Kit (ThermoFisher). Approximately 10 μg of protein was loaded per well to Mini-PROTEAN TGX Stain-Free Precast Gels (Biorad). Gels were electrophoresed at 250V for approximately 20-25 min before transfer to a nitrocellulose membrane using a Trans-Blot Turbo Transfer System (Biorad). Membranes were soaked in 4% non-fat milk dissolved in TBS-T buffer (tris-buffered saline-tritonX; Sigma-Aldrich) for “blocking” for 20 min and then incubated with

primary antibodies overnight at 4˚C on an agitating platform. Membranes were then washed four times in TBS-T for 1, 2, 4, and 5 min before being incubated with corresponding mouse or rabbit secondary antibodies for 1 hour at room temperature with agitation. Blots were washed in TBS-T four more times for 1, 2, 4, and 5 min before imaging with a ChemiDoc XRS+ System (Biorad). Images of blots produced by the Chemidoc XRS+ System were analyzed using ImageLab (Biorad) software.

qPCR

To evaluate the *HPRT1* knockout cell lines, the following primers were used:

Forward: CTCACTGTATTGCCCAGGTT

Reverse: CAGCAGGTCAGCAAAGAATTTAT

To evaluate expression of *TFAM*, the following primers were used:

Forward: AAGATTCCAAGAAGCTAAGGGTGA

Reverse: CAGAGTCAGACAGATTTTTCCAGTTT

Measurements were normalized to *ACTB* using the following primers:

Forward: ACCATTGGCAATGAGCGGTTC

Reverse: AGGTCTTTGCGGATGTCCACGT

Reverse transcription was performed using the total RNA fraction to obtain cDNA in 40 µL volume containing 1 µg of total RNA, 0.5 µg random primers, 0.5 mM dNTPs, 0.01 M DTT, and 400 U M-MLV RT (Invitrogen). Reactions were performed in 20 µL volumes on a 384-well plate either using an Applied Biosystems 7900 HT (Applied Biosystems) or a QuantStudio 6 (Thermofisher) thermocycler. The reaction mixture contained 10 µL of Power SybrGreen PCR Mastermix (Life Technologies), 1 µL of primers/probe mix, 2 µL of cDNA, and 7 µL water.

Seahorse Assays (measuring glycolysis and oxidative phosphorylation)

An XFe96 Extracellular Flux Analyzer (Agilent) was used to measure changes in oxygen consumption rate (OCR) and extracellular acidification rate (ECAR) based on the level of oxygen and on the concentration of protons in the extracellular media, respectively.

The day before the assay, approximately 30,000 HCT116 cells per well were seeded in 80 μL media in an XFe96 microplate and incubated in a 5% CO_2 incubator at 37˚C for 24 hours. On the day of the assay, 50 μL of the media was gently removed from the wells using a multichannel pipette, cells were washed twice with 100 μL XF assay medium (Agilent) and fresh XF assay medium was added. Cells were then incubated for 1 hour in a CO_2-free incubator at 37˚C for the equilibration period. The plate of cells was then transferred to the XFe96 extracellular flux analyzer and the assay was performed. One cycle involves a 2-minute mix, 2-minute wait, and 3-minute measure period. After 4 basal assay cycles, 4 cycles after each drug injection were performed.

To measure mitochondrial respiration, oligomycin (Sigma-Aldrich), FCCP and rotenone (Sigma-Aldrich) were added at specific time points to inhibit different complexes of the electron transport chain (ETC) at a final concentration of 1.5 μM, 0.5 μM and 1 μM, respectively. In the glycolytic assays, glucose (Fisher Scientific), oligomycin and 2-deoxy-D-glucose (2-DG; Sigma-Aldrich) were injected at a final concentration of 10 mM, 1.5 μM and 100 mM, respectively. Assays were performed with at least 5 replicates and normalized to cell number by performing a CyQUANT assay, as per manufacturer's recommendations.

High Performance Liquid Chromatography (HPLC)

For measuring metabolites associated with purine salvage, pentose phosphate pathway, glycolysis: media was removed and cells were washed in 5mM ammonium acetate before they were lysed in 80% methanol chilled to -20°C. Cell supernatant was dried in a Speedvac, then maintained at -80°C for less than 7 days prior to measurement. Metabolites were measured using a Thermo Scientific Ultimate 30000 UHPLC and Thermo Scientific Q Exactive Mass Spectrometer. For experiments with C13-glucose, cells were first incubated in DA NPC media substituted with C13 glucose for 4 hours, all subsequent steps were the same as described above.

For measuring dopamine, 3.4-dihydroxyphenylacetic acid (DOPAC) and homovanilic acid (HVA), cells were washed with PBS, lysed using perchloric acid, centrifuged to form pellets, and the liquid was decanted. Samples were run on an UltiMate™ 3000 CoulArray™ HPLC machine. Metabolite concentrations were quantified using OpenChrom (https://www.openchrom.net/) software. A laboratory standard sample of each compound was used to assess the concentration of each measured compound. Data was normalized based on protein concentrations. To measure the DA release in the culture media, cells were differentiated and cultured in 60mm culture dishes for 60 days. On day 60, cells were incubated in the same culture media, but supplemented with 56mM KCl for 15 minutes. HPLC was then performed as described above.

Autophagy Assay

Cells were incubated in control conditions, media starved of serum, and/or incubated in media containing 10nM Bafilomycin for 4 hours prior to lysis. All other steps were as previously described for western blot.

SUnSET Assay

DA NPC media containing 10μM of puromycin was used to incubate cells for 4 hours prior to lysis. For western blotting, protein lysates were run on Mini-PROTEAN® TGX Stain-Free™ gels and imaged under UV light as a protein loading control. All other steps were as previously described for western blot.

TUNEL cell death assay

The TUNEL Assay Kit - BrdU-Red (Abcam) was used to assess cell death. The experiment involved control and *HPRT1* KO DA NPC grown on cover slips and prepared according to the protocol provided by Abcam. First with TDT reaction buffer, TDT enzyme and BrdUTP before incubation in anti-BrdU-red antibody for 30min followed by rinsing. Each genotype was imaged 16 times on an Axio Imager (Zeiss). DAPI nuclei were quantified in QuPath using cell detection. BrdUTP-positive nuclei (red) were counted manually.

Quantification of cilia

To count cilia, first ImageJ was used to convert Z-stacks of images from the Axio Imager (Zeiss) were converted to max projections. Nuclei and cilia were quantified using QuPath. The cell detection feature was used whenever possible to automatically quantify nuclei stained with DAPI. When cilia were stained for Acetylated tubulin (green) and IFT88 (red), cilia were defined as a bright green length capped at both ends by red dots. When cilia were stained for ARL13B (red), bright red dots/lines were considered as cilia. For each image, the proportion of ciliated nuclei was calculated. For measuring the length of cilia imaged, IMARIS software was used to render Z-stacks of two-dimensional images into three-dimensional volumes. Length of cilia was defined as the shortest possible distance between both ends in the three-dimensional volume.

Chapter 3: "Lesch-Nyhan disease causes impaired energy metabolism and reduced developmental potential in midbrain dopaminergic cells"

[Reproduced from Stem Cell Reports (Bell et al. 2021)*]*

Scott Bell,1,2,10 Vincent McCarty,1,2,10 Huashan Peng,1,2 Malvin Jefri,1,2 Nuwan Hettige,1,2 Lilit Antonyan,1,2 Liam Crapper,1,2 Liam A. O'Leary,1,2 Xin Zhang,1,2 Ying Zhang,1,2 Hanrong Wu,1,2 Diane Sutcliffe,3,4,5 Ilaria Kolobova,1,2 Thad A. Rosenberger,6 Luc Moquin,2 Alain Gratton,2 Jelena Popic,7,8 Ilse Gantois,7,8 Patrick S. Stumpf,9 Andreas A. Schuppert,9 Naguib Mechawar,2 Nahum Sonenberg,7,8 Michel L. Tremblay,7,8 Hyder A. Jinnah,3,4,5 and Carl Ernst1,2,*

1 Psychiatric Genetics Group, McGill University, Montreal, QC, Canada

2 Department of Psychiatry, McGill University and Douglas Hospital Research Institute, 6875 LaSalle Boulevard, Frank Common Building, Room 2101.2, Montreal, QC H4H 1R3, Canada

3 Department of Neurology, Emory University, Atlanta, GA, USA

4 Department of Human Genetics, Emory University, Atlanta, GA, USA

5 Department of Pediatrics, Emory University, Atlanta, GA, USA

6 Department of Pharmacology, Physiology, and Therapeutics, School of Medicine and Health Sciences, University of North Dakota, Grand Forks, ND, USA

7 Department of Biochemistry, McGill University, Montreal, QC, Canada

8 Rosalind and Morris Goodman Cancer Research Centre, McGill University, Montreal, QC, Canada

9 Joint Research Center for Computational Biomedicine, RWTH Aachen University, Aachen, Germany

10 These authors contributed equally

*Correspondence: carl.ernst@mcgill.ca

https://doi.org/10.1016/j.stemcr.2021.06.003

Stem Cell Reports | Vol. 16 | 1749–1762 | July 13, 2021

GRAPHICAL ABSTRACT

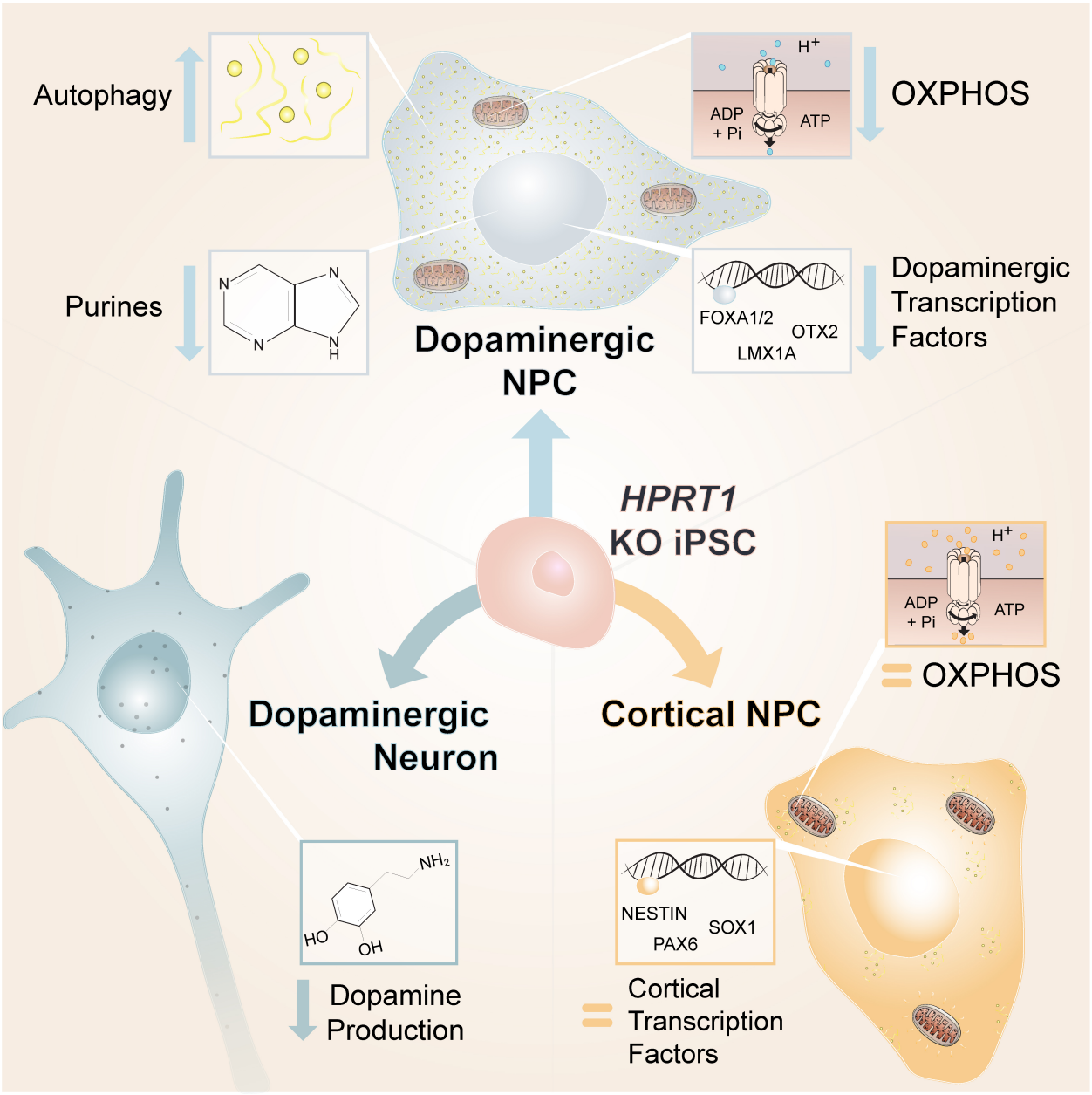

SUMMARY

Mutations in *HPRT1*, a gene encoding a rate-limiting enzyme for purine salvage, cause Lesch-Nyhan disease which is characterized by self-injury and motor impairments. We leveraged stem cell and genetic engineering technologies to model the disease in isogenic and patient-derived forebrain and midbrain cell types. Dopaminergic progenitor cells deficient in HPRT showed decreased intensity of all developmental cell-fate markers measured. Metabolic analyses revealed significant loss of all purine derivatives, except hypoxanthine, and impaired glycolysis and oxidative phosphorylation. real-time glucose tracing demonstrated increased shunting to the pentose phosphate pathway for *de novo* purine synthesis at the expense of ATP production. Purine depletion in dopaminergic progenitor cells resulted in loss of RHEB, impairing mTORC1 activation. These data demonstrate dopaminergic-specific effects of purine salvage deficiency and unexpectedly reveal that dopaminergic progenitor cells are programmed to a high-energy state prior to higher energy demands of terminally differentiated cells.

INTRODUCTION

Lesch-Nyhan disease (LND) is a rare genetic condition characterized by severe motor impairment, dystonia, crystals in the urine, and self-mutilation (Jinnah et al., 2006; Lesch and Nyhan, 1964). It is caused by sequence errors in *HPRT1*, which encodes the protein hypoxanthine-guanine phosphoribosyl transferase (HPRT), a critical enzyme in purine recycling. HPRT adds a phospho-ribose group to breakdown products of purine metabolism, guanine or hypoxanthine, and converts these to guanosine monophosphate (GMP) or inosine monophosphate (IMP), respectively. Deficiency of HPRT presents as a ‘‘spectrum disorder,’’ with only those with enzymatic activity under ~2% showing behavioral and neurological impairment, including self-injury and motor anomalies. Those with enzymatic activity greater than 2% are called LN variants (LNVs) or ‘‘attenuated variants’’ (Jinnah et al., 2010). These cases are subcategorized into those with hyperuricemia (greater than ~8% enzymatic activity) or those with hyperuricemia and neurological dysfunction but no self-injury (>1% enzymatic activity) (Jinnah et al., 2010). Since *HPRT1* is located on the X chromosome, both LND and LNV follow an X-linked recessive pattern of inheritance and thus present almost exclusively in boys.

Previous research into LND has used a variety of models, both in vivo and in vitro (Bell et al., 2016). *In vitro* studies used accessible somatic cells from outside the central nervous system, such as fibroblasts (Costa et al., 1980; Cox et al., 1970; Edelstein et al., 1978; Jinnah, 2009), which were informative on the nature of genetic variants leading to LND but provided limited information about the neurological changes that underpinned its most dramatic symptoms (Costa et al., 1980). A more clinically relevant model of Lesch-Nyhan spectrum disorders would ideally be made in neuronal cells, a technique now available (Takahashi et al., 2007), which may help to answer long-standing questions in LND research.

Beyond the genetic mutations in *HPRT1*, the pathogenesis of LND remains unknown, although there exist clinical, human neuroanatomical, and mouse knockout (KO) studies suggesting midbrain dopaminergic cell involvement. Positron emission tomography imaging and postmortem brain studies have indicated that the brains of LND patients are broadly normal, but show significantly reduced dopamine and tyrosine hydroxylase (TH) levels (Ernst et al., 1996; Göttle et al., 2014; Watts et al., 1982). Postmortem data suggest that cell markers of midbrain dopaminergic cell identity are present in midbrain basal ganglia cells but at decreased intensity levels, without a morphological correlate; that is, cell number, density, and appearance look grossly normal (Göttle et al., 2014). This observation and others led to a ‘‘developmental’’ hypothesis of LND (Egami et al., 2007; Lewers et al., 2008), whereby purine salvage may be required at some stage during midbrain dopaminergic cell development for these cells to terminally differentiate.

Cell models used to investigate the neurobiology of LND have been HPRT-deficient cancerous cell lines obtained from human brain tumors. These lines were able to recapture many aspects of human neural biology and predicted HPRT dysfunction, such as a reduction in dopamine (DA) production (Bitler and Howard, 1986) and dopaminergic differentiation (Yeh et al., 1998); however, immortalized cell lines were also found to possess qualities that confounded the results because of their variable genomes (Paul et al., 2007) and unstable differentiation into the dopaminergic lineage (Gao et al., 2016). Rodent *HPRT1* KO studies have shown little to no behavioral phenotype, but significant decreases in DA levels in the midbrain (Jinnah, 2009). Cells produce purines by synthesizing them *de novo* or by recycling breakdown products, the latter of which is dependent on HPRT. In *de novo* purine synthesis, and beginning from cellular glucose uptake, glucose derivatives are shunted via the pentose phosphate pathway (PPP) (Pedley and

Benkovic, 2017) to become 5-carbon pentose sugars such as ribose-5-phosphate (R5P) (Pedley and Benkovic, 2017), which can then be used for other cellular needs, including purine synthesis. The first committed steps from a pentose sugar into the series of reactions that make up purine synthesis is that from R5P to phosphoribosyl diphosphate (PRPP). PRPP enters a series of enzymatic reactions requiring inputs such as glutamine, ATP, and folate derivatives (Moffatt and Ashihara, 2002), and generates several intermediate products such as 5-aminoimidazole- 4-carboxamide ribonucleotide (AICAR). The final product of the *de novo* purine synthesis pathway, IMP, is readily converted to GMP or AMP. These ribonucleotide products are widely used in the cell for a variety of purposes, including DNA/RNA synthesis and energy storage via production of ATP and GTP. Eventually, adenine and guanine may be degraded into hypoxanthine and xanthine. If no HPRT-dependent recycling occurs, these waste metabolites are secreted as uric acid (Moffatt and Ashihara, 2002).

Cells have different energy sensors to cope with changing energy states. One important sensor is AMP-activated protein kinase (AMPK), which senses the ratio of AMP to ATP; an increased ratio activates the enzyme to drive other metabolic pathways to increase ATP (Garcia and Shaw, 2017). The mTORC (mammalian target of rapamycin complex) axis is a signaling pathway that can integrate grTCowth factor/second messenger signals (e.g., FGF/EGF-PI3-AKT) and cell nutrient status (e.g., purines and amino acids) to affect cell growth, ribosome synthesis, autophagy, ciliary dynamics, and protein translation (Emmanuel et al., 2017; Saxton and Sabatini, 2017). One key brake on mTORC1 is the TSC1/2 complex, which inhibits the activation of the mTORC1 activator RHEB (Hoxhaj et al., 2017). RHEB is a purine sensor; a loss of purines depletes RHEB, reducing mTORC1 activation (Emmanuel et al., 2017). mTORC1 is associated with cell differentiation and promotes cell maturation. Engineered mutations in the *Mtor* gene cause

embryonic lethality in mice (Murakami et al., 2004), and selective deletion in brain causes major brain alterations (Garza-Lombo´ and Gonsebatt, 2016; Ka et al., 2014), including deficits in progenitor cell self-renewal. Across other cell types, induced mutations impairing mTORC1 lead to loss of differentiation potential (La et al., 2018; Wang et al., 2016), suggesting that activation of mTORC1 may be important in allowing cells to develop to their full potential. Here we address long-standing questions about HPRT deficiency in the human nervous system. We find that loss of HPRT has remarkably selective effects in midbrain dopaminergic cells, specifically in reduced ATP production and decreased mTORC1 activation. These effects may drive developmental loss of expression in critical genes such as *FOXA1/2* needed for dopaminergic cell terminal differentiation.

RESULTS

Simultaneous generation of midbrain dopaminergic and forebrain cortical progenitor cells reveals dopaminergic cell-specific effects of purine salvage deficiency on expression of essential developmental markers

We made two different clonal *HPRT1* KO lines, both isogenic with a single healthy donor line (Figures S1A and S1B), using our simultaneous reprogramming/gene editing technique (Bell et al., 2019). We used two separate induced pluripotent stem cell (iPSC) clones from this donor cell and refer to these clones as control 1 and control 2. Upon reaching a pluripotent state, iPSCs were assessed for markers of pluripotency in both KO and control states, and we observed no differences in ability to make iPSCs or marker intensity across cell lines (Figures S1C and S1D). Loss of HPRT thus has no effect on stem cell induction or maintenance of iPSCs, despite clear expression of HPRT in this cell type. All iPSCs were assessed for genomic integrity using a next-generation sequencing assay of 5,209 genes, found approximately equally across chromosomes. The resolution of detection for chromosomal anomalies was R10 Mb. Next, we simultaneously differentiated each iPSC line independently to distinct populations of midbrain DAergic (DA) and forebrain cortical (CN) neural progenitor cells (NPCs), using gold standard assays that we have previously published for each cell type (Bell et al., 2019; Jefri et al., 2020). Simultaneous differentiation allows us to control for operator, time-of-day, and media batch effects of common reagents used to derive CN or DA NPCs from iPSCs. Quality control parameters include staining both NPC types and 30-day-differentiated cells with markers for both CN and DA cells relevant to each time point (Figure S2). The DA marker FOXA2 stained exclusively DA NPCs, while TH was found only in differentiated DA neurons (Figures S2A and S2B). FOXG1 was absent from midbrain cells but present in both CN NPCs and CN neurons (Figures S2C and S2B).

Electrophysiological properties of DA neurons showed characteristic features of midbrain DA cells, including high-frequency bursting activity (Figure S2E) and a depolarizing sag in response to current clamp hyperpolarization followed by action potential trains (Figure S2F). Direct immunocytochemical comparison of both CN and DA NPCs made simultaneously for both *HPRT1* KO and isogenic controls revealed unambiguous decreases in intensity of all DA markers in *HPRT1* KOs, although all markers were detected in almost all cells (Figures 1A–1E). Quantification by western blot and using an expanded range of markers further supported this finding (Figure 1F; FOXA1, 73% ± 11% [p = 0.0098] decrease; FOXA2, 76% ± 8.6% [p = 0.0074] decrease; LMX1A, 34% ± 10% [p = 0.0408] decrease). Assessment of cell death showed slight but significantly less cell death (Figures S3A and S3B) in KO cells. We found no discernible difference for *HPRT1* KO in CN NPCs for any markers, suggesting that loss of HPRT may lead to relatively specific effects in DA NPCs. Such drastic decreases in the intensity of DA markers in this committed progenitor cell type suggests that loss of HPRT affects early stages of developmental programming in DA cells but not CN cells. The detection of DA markers with less intensity in *HPRT1* KO suggests that cell fate has not changed, but rather commitment to the midbrain DA NPC lineage may be impaired.

The significant decrease in intensity of DA markers in NPCs suggests that HPRT has a specific role in programming dopaminergic cell fate. If this is the case, we would expect that markers of more differentiated DA cells should show significant defects as well, since expression of mature markers is dependent on full expression of NPC markers such as Nurr1 (NR4A2) (Saucedo-Cardenas et al., 1998) and FOXA1/2 (Ferri et al., 2007), which continue to be expressed in more mature DA neurons. We differentiated DA NPCs for 30 days and performed immunocytochemistry (ICC) against TH and the mature neuronal stain TUJ1 (Figure 2A). An

automated analysis of signal intensity across 13,271 imaged cells found an average TH signal reduction of 50.6% ($p << 0.05$) (Figure 2B).Western blot showed clear decreases in TH (down 67% ± 14%, $p = 0.0168$) (Figure 2C) and supported this finding quantitatively using an expanded set of markers (FOXA1, down 60% ± 13% [$p = 0.00267$], FOXA2, down 73% ± 9.6% [$p = 0.0051$], and LMX1A, down 45% ± 15% [$p = 0.0432$]). While we do detect weak TH staining in many cells without HPRT, fewer cells are TH positive than would be expected from the NPC marker stage, where almost all cells are positive for DA markers (but with less intensity). These data suggest that the decreased intensity of DA NPC cell-fate markers might alter cell-fate programming as NPCs mature and differentiate.

The decreased expression of TH should be reflected in the amount of dopamine that *HPRT1* KO cells produce. To test this hypothesis, we performed high-performance liquid chromatography (HPLC) measurements of dopamine and breakdown products of dopamine at 25 and 80 days of differentiation from DA NPCs (Figures 2D–2G). We found significant decreases in dopamine and derivatives of dopamine in *HPRT1* KO neurons, which were exasperated as cells aged, likely reflecting the increase in DA production that occurs as these cells mature between 25 and 80 days. Given the potential cell-fate change at later developmental

stages, but clear expression of DA markers at NPC stages, we opted to perform further studies in the NPC stage, reasoning that later stage outcomes are derivatives of early cell-fate problems.

Loss of adenosine and guanosine derivatives in dopaminergic cells is more pronounced than in cortical cells

Loss of HPRT prevents salvage of purines, which could ultimately lead to a lack of purine derivatives, including ATP and GTP (Figure 3A). To assess and compare the direct effects of

HPRT deficiency in isogenic stem, cortical, and midbrain cells, we performed HPLC after metabolite extraction (Figure 3). First, we observed that both KO CN NPCs and KO DA NPCs exhibit large increases (~4-fold) in hypoxanthine, an expected consequence of HPRT deficiency observed in patients with LND across cell types (Fu et al., 2015). No such effect was seen in KO iPSCs, where HPRT is detectable; however, we cannot rule out increased hypoxanthine excretion to the cell culture medium, as has been reported in stem cells (Sutcliffe et al., 2021). With respect to adenosine and guanosine derivatives, we observed decreased levels of almost all metabolites in HPRT-deficient NPCs, with consistently higher levels detected in DA cells than in CN, even independent of HPRT deficiency (Figures 3B and 3C). iPSCs had consistently lower levels of purine metabolites than DA or CN NPCs and showed no decrease in purine levels when *HPRT1* was deleted, consistent with hypoxanthine concentrations. These data provide evidence that DA progenitors, morphologically indistinguishable from CN progenitors, have higher metabolic rates than forebrain cells, given higher baseline levels of adenine and guanine derivatives, even in healthy cells. This is surprising because midbrain DA cells are thought to have higher metabolic rates, due to pacemaker activity, and extensive connectivity (Mamelak, 2018; Pacelli et al., 2015), which are properties of terminally differentiated cells. This suggests that DA cells might be programmed very early on to have higher metabolic rates prior to cell maturation consisting of highly arborized morphology and pacemaker activity.

Significant loss of glycolysis and oxidative phosphorylation potential due to HPRT deficiency

To assess the effects of HPRT deficiency on metabolism in DA and CN cells, oxidative phosphorylation (OXPHOS) and glycolytic potential (Figure 4A) were evaluated after drug

challenge in real time. To this end, we simultaneously measured both oxygen consumption and extracellular acidification in genotypically matched DA and CN NPCs (Figures 4B and 4C). Consistent with our metabolite HPLC data, we found that control CN NPCs are less metabolically active than control DA NPCs, and that *HPRT1* defects in DA cells significantly impair both glycolysis and OXPHOS. In CN NPCs, we detected a significant decrease in glycolysis, but not OXPHOS (Figures 4B and 4C). This impairment may be due to the specific increased metabolic needs in DA NPCs, which cannot be met without purine salvage. The abundance of mitochondria in a cell can fluctuate with energy state and have a significant impact on cellular metabolism (Liesa et al., 2009). We examined *TOMM20* expression, which is used as a marker of mitochondria, in DA NPCs and found no qualitative differences between *HPRT1* KO and isogenic controls (Figure S3C). This was supported by unchanged expression of *TFAM* RNA, a key mitochondrial transcription factor, in HPRT-deficient

compared with isogenic control DA NPCs (Figure S3D). We conclude that OXPHOS is specifically affected in DA NPCs lacking HPRT and that this is unlikely to be due to physiological changes in mitochondria.

More glucose shunted to the pentose phosphate pathway (PPP) and increased *de novo* purine synthesis in HPRT-deficient DA cells

The loss of glycolysis and OXPHOS potential might reflect increased utilization and flux of glucose to the PPP to create new purines at the expense of glycolysis and OXPHOS. We measured several metabolites known to be important in DA NPCs to determine if the PPP (Figure 4A) is more active in HPRT-deficient DA NPCs. We found increased levels of R5P and PRPP and AICAR, an intermediate product in *de novo* purine synthesis (Figure 4D). We also assessed AMP

and IMP levels and included a measure of lactate as a readout for glycolytic flux. Lactate levels were decreased in HPRT-deficient cells, and levels of AMP and IMP (Figure 4D) were consistent with our previous results. This supports a hypothesis where glucose is shunted to a 5-carbon sugar to make purines, possibly at the expense of glycolysis and OXPHOS. Glucose can also be utilized to create glycoproteins via the glycosylation pathway (Reily et al., 2019). We assessed glycoprotein synthesis to determine if glycosylation rate was affected by HPRT deficiency, but we detected no significant change in glycosylation state in HPRT-deficient DA and CN NPCs (Figures S4A and S4B).

To unequivocally demonstrate increased shunting of glucose to the PPP in HPRT-deficient DA NPCs, we exposed cells to a 13C-glucose medium for 4 h before extracting metabolites. This allows tracking of any metabolites that incorporate 13C. We found increased 13C in the R5P, PRPP, and AICAR metabolite pools in HPRT-deficient DA NPCs compared with control DA NPCs (Figure 4E). HPRT-deficient DA NPCs also had less 13C-containing lactate than isogenic control DA NPCs, a measure of glycolysis (Figure 4E). Finally, we found that levels of 13C in AMP and IMP were increased in HPRT-deficient DA NPCs compared with isogenic controls, suggesting a model whereby glucose is shunted to the PPP at the expense of energy metabolism and where the higher rate of *de novo* synthesis in HPRT-deficient DA NPCs is not sufficient to restore purine levels to baseline conditions (Figures 2D and 2E).

Inhibition of mTORC1 in HPRT-deficient dopaminergic cells but not cortical cells

We next sought to characterize the response of metabolic sensors to these metabolic imbalances. We investigated RHEB, a sensor of purine levels in cells (Hoxhaj et al., 2017) and required driver of mTORC1 (Figure 5A). HPRT deficiency strongly reduced RHEB levels in DA

NPCs, but not in iPSCs or CN NPCs (Figure 5B), showing remarkable cell-type selectivity. If RHEB is indeed a purine sensor, this result suggests that only DA NPCs deficient in HPRT have purine loss drastic enough to trigger this sensor and impair mTORC1 as a result, possibly due to higher energy demands in DA NPCs. To test this, we selected two output markers of mTORC1 activity, ULK1 and RPS6, both of which are commonly used to monitor mTORC1 activity (Yanagiya et al., 2012). HPRT-deficient DA NPCs showed reduced levels of phosphorylation in ULK1 at residue 757 (Figure 5B), an exclusive target of mTORC1 (Chan et al., 2009). Because of the association between mTORC1, sonic hedgehog (SHH) signaling via GLI2, and dopaminergic cell development (Wu et al., 2017; Yan et al., 2016), we also examined if GLI2 levels were decreased in DA NPCs. Since less mTORC1 activation leads to less p757-ULK1, and phosphorylation of this site removes the brake on autophagy, we wanted to confirm that autophagy was increased with a real-time autophagy assay, involving starvation and autophagosome formation blockade by bafilomycin A in living cells (Figure 5C). In HPRT-deficient DA NPCs, we observed increased LC3-II (lower band) under autophagosome blockade, starvation only, and both starvation and autophagosome blockade together. This suggests that both baseline autophagy and starvation-induced autophagy are increased with HPRT deficiency, an effect that could be triggered by the depletion of RHEB and subsequent loss of mTORC1 activity.

Ribosomal protein S6 is downstream of mTORC1 and it can be activated by phosphorylation at position 240/244 (Meyuhas, 2015) (Figure S4C). Despite cell-line-specific variation, triplicate Western blot analysis detected a significant drop in 240/244 phosphorylation in DA NPCs, but not in CN NPCs (Figures 5D and S4D). These data support the idea that mTORC1 is less active when HPRT is deficient in DA NPCs. Ribosomal protein S6 is associated with protein synthesis of particular mRNAs (Meyuhas, 2015), so we attempted a real-time protein synthesis assay using the

SUnSET assay (Schmidt et al., 2009). *HPRT1* KO DA NPCs failed to show any significant difference in protein synthesis (Figure 5E), although this may be due to reported ambiguous p240/244-S6 effects on translation (Biever et al., 2015).

We were intrigued by the data suggesting increased autophagy via the decreases in p757-ULK1. Autophagy is reported to affect cilia, a signaling organelle for SHH required for DA cell development (Hynes et al., 1995). Autophagy is necessary for cilia growth, and ciliary signaling appears to affect autophagy (Pampliega and Cuervo, 2016). It is theoretically possible that autophagy affects DA cell development by influencing cilia length and frequency. To test this hypothesis, we measured cilia length and occurrence throughout the development of iPSCs into DA NPCs (Figure S5A) by visualizing cilia using combined IFT88 and acetylated tubulin, as well as ARL13B (Figure S5B). We found no evidence of significant difference in either cilia length or the proportion of ciliated cells at any developmental time point assessed (Figures S5C and S5D). These data suggest cilia dynamics are normal during differentiation from stem cells to DA NPCs and may suggest that the DA-specific deficiencies caused by HPRT loss begin once cells are in a purified, committed, and higher energy DA progenitor state.

AMPK is a sensor of the AMP/ATP ratio and suppresses mTORC1 via phosphorylation of RAPTOR and TSC2 (Cork et al., 2018). As ATP levels drop and AMP levels rise, AMPK undergoes a conformational change, by the replacement of ATP by AMP in the active site of AMPK. This event leads to increased phosphorylation of residues Thr 172 and Thr 183 of AMPK, allowing the kinase to become active to restore ATP levels (Figure S6A). We have found that HPRT deficiency in DA NPCs leads to proportional decreases in ATP and AMP (Figure S6B, derived from data in Figure 3B), which might suggest that AMPK is not activated, even in the case of the severe loss of ATP in HPRT deficiency. That said, exogenously applied AICAR, which is

high under our conditions, is a commonly used stimulator of AMPK (Sun et al., 2007) and is of interest because of its transformation to 5-amino-1-b-D-ribofuranosylimidazole-4-carboxamide monophosphate (ZMP), which has been associated with LND (Sidi and Mitchell, 1985). To assess this idea, we measured both p172/183 in AMPK and its target site in RAPTOR (Ser 722/792) (Gwinn et al., 2008) from HPRT KO DA NPCs and controls (Figures S6C–S6E). We found no difference in AMPK or RAPTOR phosphorylation states, meaning that AMPK does not affect energy deficits via mTORC1 or otherwise in DA NPCs deficient in HPRT.

Eight Lesch-Nyhan disease and variant cases recapitulate the effects of HPRT deficiency on cell-fate marker expression and OXPHOS

To externally validate the *HPRT1* KO data in people affected with disease and to demonstrate molecular effects on different genetic backgrounds, we made DA NPCs from three LND subjects, five LNV subjects, and four controls (Table S1) (Figure 6A). To minimize variability, the 12 fibroblast cell lines were reprogrammed to iPSCs simultaneously and then immediately differentiated to dopaminergic NPCs and neurons, when they were evaluated for metabolic effects and markers of dopaminergic fate.

A metabolic screen of PPP metabolites, identical in design to the KO studies, showed significant effects in all metabolites assessed in LND cells, with LNV cells showing an intermediate molecular phenotype between control and LND (Figure 6B). We found significant decreases in OXPHOS output measures in DA NPCs derived from HPRT-deficient subjects, with LNV subjects showing OXPHOS rates approximately intermediate to LND subjects and controls, accordant with the level of HPRT enzymatic activity but in a non-linear relationship (Figures 6C–6E). Finally, we found reduced protein levels of DA NPC markers and mTORC1 outputs in LND

and LNV DA NPCs (Figure 6F). The expression of DA markers in LND-derived NPCs compared with controls showed deficits in FOXA1 (78% ± 6% reduction compared with controls, $p \leq 0.0001$), FOXA2 (63% ± 15%, $p = 0.0007$), LMX1A (75% ± 19%, $p = 0.0178$), and GLI2 (59% ± 10% $p \leq 0.0004$). Reduction in markers for LNV and LND samples were consistent with a one-phase decay exponential relationship, suggesting that most of the effect of HPRT deficiency on the expression of these proteins occurs as HPRT approaches complete loss (Figure 6G), providing in vitro support for why <1% activity might lead to such a severe clinical outcome compared with enzymatic activity greater than 2%; that is, the effect of HPRT loss on OXPHOS and DA markers is not linear. We differentiated all NPC lines from all three groups ($n = 12$) for 30 days and then performed Western blot for mTORC1 and DA markers in neurons (Figure 6H) and plotted these against HPRT enzymatic activity (Figure 6I). We observed relationships similar to what we found in DA NPCs, that is, less HPRT activity corresponded with fewer DA markers in neurons and less mTORC1 activity, and this relationship is non-linear except for TH and ULK1. The presence of these deficits in post-mitotic cells suggests deficits persist throughout development once in place in NPCs.

DISCUSSION

Our data suggest that cell-type-specific experiments are essential to investigate HPRT dysfunction, since the intrinsic energy state may determine whether *de novo* synthesis can compensate for purine salvage loss. A specific threshold of energy impairment may need to be reached before a cell's developmental fate is compromised. DA cells have a higher background metabolic rate than CN cells and expose HPRT impairments as problems in energy metabolism, which can be obscured in cells without high-energy states. This was surprising because the high metabolic rates observed in midbrain DA cells uncovered in studies of Parkinson's disease have long been thought to be due to processes seen only in mature, post-mitotic cells (Mamelak, 2018; Pacelli et al., 2015). Our data show that DA cells are developmentally programmed for higher metabolic rates prior to any neurite branching and in the presumed absence of autonomous cell firing. It therefore seems probable that the programming of this metabolic activity may allow for the development of the energy-intensive processes seen in mature ventral midbrain DA cells, rather than vice versa.

Our investigation into glucose usage clarifies several long-standing questions for purine salvage deficiency studies. First, our data show that glucose is shunted to the PPP to increase *de novo* purine synthesis and that this is done at the expense of glycolysis and OXPHOS. We detected no changes in glycosylation levels, which suggests that that system likely remains intact. Our 13C tracer experiments reveal that there are more purines being produced in HPRT-deficient DA cells, but that this level is not sufficient to compensate for the loss of purine salvage. While the cell may bring in more glucose, shunting glucose to *de novo* synthesis might remove product from the glucose budget and negatively affect glycolysis and OXPHOS. Loss of purine salvage results in significant deficits in midbrain DA progenitor glycolysis and OXPHOS, with cortical cells

displaying only slight but significant deficits in glycolysis. This result may suggest that HPRT deficiency compromises the energy state of DA NPCs by reducing the ability of the cell to maintain an appropriately high level of OXPHOS.

DA progenitor cells likely sense the metabolic changes brought on by HPRT deficiency at least in part through the purine sensor RHEB, an obligate activator of mTORC1 (Emmanuel et al., 2017; Hoxhaj et al., 2017). RHEB is significantly depleted in HPRT-deficient cells, a result that has been shown in other experimental systems when purines are absent (Hoxhaj et al., 2017). This implies that mTORC1 cannot be fully activated, which may be important to drive DA cell differentiation. For example, in pancreatic cells mTORC1 is dispensable for a cell development but is essential for a cell maturation (Bozadjieva et al., 2017), which is driven by mTORC1 via FOXA2 and transcription of *ABCC8* (*Sur1*) and *KCNJ11* (*Kir6.2*), all of which are also markers of dopaminergic cells of the midbrain (Osborn and Hallett, 2017). These data suggest that mTORC1 activation is important for cell differentiation and activation of FOXA2, and also that mTORC1 has a role in midbrain dopaminergic cells, although we cannot rule out mTORC1 being a passenger of some other as of yet unidentified driver effect.

The loss of DA markers correlates with the degree of loss of enzymatic activity of HPRT, suggesting a strong association between purine salvage and midbrain cell development.

While no single marker is definitive of midbrain DA cells, analysis of all suggests that purine salvage must be intact for proper differentiation of this cell type. It is tempting to speculate that the deficits in OXPHOS and ATP production we observed early on in DA programming lead to the loss of marker potential, but we warn against this simplistic interpretation. We cannot rule out that the DA markers drive the metabolic deficits, or that the two processes are intertwined. *FOXA1/2* (aka *HNF3a/b*), for example, are well known glucose-response genes in the pancreas

(Heddad Masson et al., 2014) and are essential for DA development according to mouse KO studies (Gao et al., 2010). Indeed, mouse *FOXA1/2* KO shows reduced TH staining with variable loss of DA cells (Pristera` et al., 2015), a situation very similar to what is observed in postmortem LND brains (Go¨ttle et al., 2014).

CONCLUSION

The heightened energy state of DA progenitor cells may be restricted by some feature or constellation of proteins observed in stem cells, hindering differentiation of DA NPCs due to the inability to shift from *de novo* synthesis to purine salvage. Preserving or reverting to a ‘‘stem-like’’ state might ensure enough purines for a cell by relying on *de novo* synthesis, but these stem cell proteins might also inhibit differentiation, which could explain why DA NPCs still meet criteria for DA NPCs, but with less intense staining. Decreased cell death with HPRT loss may also be a feature of cells more reliant on *de novo* synthesis rather than salvage. Precisely what DA NPCs deficient in HPRT become after terminal differentiation is not currently known, although we favor a surrounding cell type of the substantia nigra such as red nucleus cell subtypes.

EXPERIMENTAL PROCEDURES

Tables S1–S3 in the supplemental information outline the cell lines and antibodies used in this study. This work was approved by the research ethics board by the Douglas Hospital Research Institute.

CRISPR-Cas9 generation of *HPRT1* knockout

A double-nickase CRIPSR-Cas9 gene editing system with gRNA (DNA2.0) targeting a 13 bp exonic sequence of *HPRT1* (AGTCCTA CAGAAATAAAATC) was generated with a Paprika RFP reporter (DNA 2.0). Five micrograms of this construct was added per transfection reaction, and transfection was carried out using the parameters described for iPSC induction. Following transfection, the cells were plated on Matrigel-coated plates in 10% FBS DMEM for 24 h. The cells were then detached and sorted via fluorescence-activated cell sorting for RFP+ cells. RFP+ cells were then replated on Matrigelcoated plates in 10% FBS DMEM supplemented with 2 mg/mL puromycin. Following 48 h of selection, the cells were dissociated using 0.05% EDTA-trypsin and plated in Matrigel-coated six-well tissue culture plates (Corning) in TesR-E7 medium at a density of ~1,000 cells per well. Colony formation, picking, and purification proceeded as described for iPSC induction.

Reprogramming to induced pluripotent stem cells

Fibroblasts were cultured in DMEM (Invitrogen) supplemented with 10% BSA (Invitrogen). The cells were then reprogrammed using episomal reprogramming vectors containing Oct4, Sox2, Myc3/4, Klf4, ShRNA P53 (ALSTEM), and a puromycin-resistance gene using the Neon transfection system (Invitrogen). Following transfection, the cells were plated on tissue culture

plates coated with Matrigel (Corning) in TesR-E7 medium (STEMCELL Technologies) supplemented with 2 mg/mL puromycin (Sigma). After 48 h of puromycin selection, fresh TesR-E7 medium was provided, until distinct and robust iPSC colonies formed, at which point mTESR1 medium (STEMCELL Technologies) was used to maintain and proliferate the colonies.

Induction of iPSCs to neural progenitor cells

iPSC colonies were dissociated and resuspended in DMEM/F12 medium supplemented with N2 (Invitrogen), B27 (Invitrogen) and BSA (1 mg/mL), Y27632 (10 mM; AdooQ Bioscience), SB431542 (10 mM; Selleckchem), and Noggin (200 ng/mL; GenScript) onto non-adherent plates to form organoids. After 1 week of maintenance as organoids, the cells were dissociated and plated on Matrigel- coated plates in DMEM/F12 supplemented with B27, bFGF (20 ng/mL), EGF (20 ng/mL), and laminin (1 mg/mL) for a further 7 days of differentiation, with the medium exchanged every 3 days. Cells were assessed for NPC morphology and stained for markers of forebrain NPCs (PAX6, SOX2, TUJ1) and OCT4.

Differentiation of NPCs to post-mitotic neurons

Differentiation was initiated when NPCs reached 70% confluency. Medium was exchanged for DMEM/F12 supplemented with B27, GDNF (2 mM, GenScript), BDNF(1 mM, GenScript), and laminin (1 mg/mL). Cells were maintained in this medium, with half the medium exchanged every 2 days until the cells achieved the desired developmental time point.

Quantification of cell identities (immunocytochemistry)

ICC quantification of Nurr1 (NR4A2), FOXA2, OTX2, and TH was performed using QuPath, with data collected from 32 images for each analysis. For each image, cell areas were defined using cell detection in the DAPI channel. The mean signal intensity (value between 0 and 255) within the area defined by cell detection was recorded for each image. An overall average across the 16 images from each genotype was determined. Analyses for Nurr1 and FOX2 in DA NPC involved mean signal intensity measurements from 3,719 detected cells. The analysis for OTX2 in DA NPC involved mean signal intensity measurements from 4,634 detected cells. The analysis for TH in neurons involved mean signal intensity measurements from 13,271 detected cells.

SUPPLEMENTAL INFORMATION

Supplemental information can be found online at https://doi.org/10.1016/j.stemcr.2021.06.003.

AUTHOR CONTRIBUTIONS

S.B., V.M., and C.E. wrote the manuscript and were involved in all aspects of the design and execution of the study. H.P., M.J., N.H., L.A., L.C., L.A.O., X.Z., Y.Z., H.W., and I.K. performed experiments. D.S., N.M., and H.A.J. contributed reagents and advised on study design; T.A.R., L.M., and A.G. performed HPLC. J.P., I.G., and N.S. performed and interpreted protein assays related to mTORC1; P.S.S. and A.A.S. performed statistical analyses. M.L.T. coordinated and supervised the Seahorse experiments.

ACKNOWLEDGMENTS

Robert Flick at the University of Toronto's BioZone facility performed all metabolic analyses. Daina Avizonis and Gaelle Bridon established pilot metabolic data at McGill facilities. Jeff Gross and LifeLabs Genetics performed genomic integrity analysis. All images were taken at the Molecular and Cellular Microscopy Platform at the Douglas Hospital Research Center. C.E. is funded by a Canada Research Chair and this work was supported in part by the CIHR. This work was also supported in part by NIH R56 NS102980 and R01 NS109242.

Figure 1

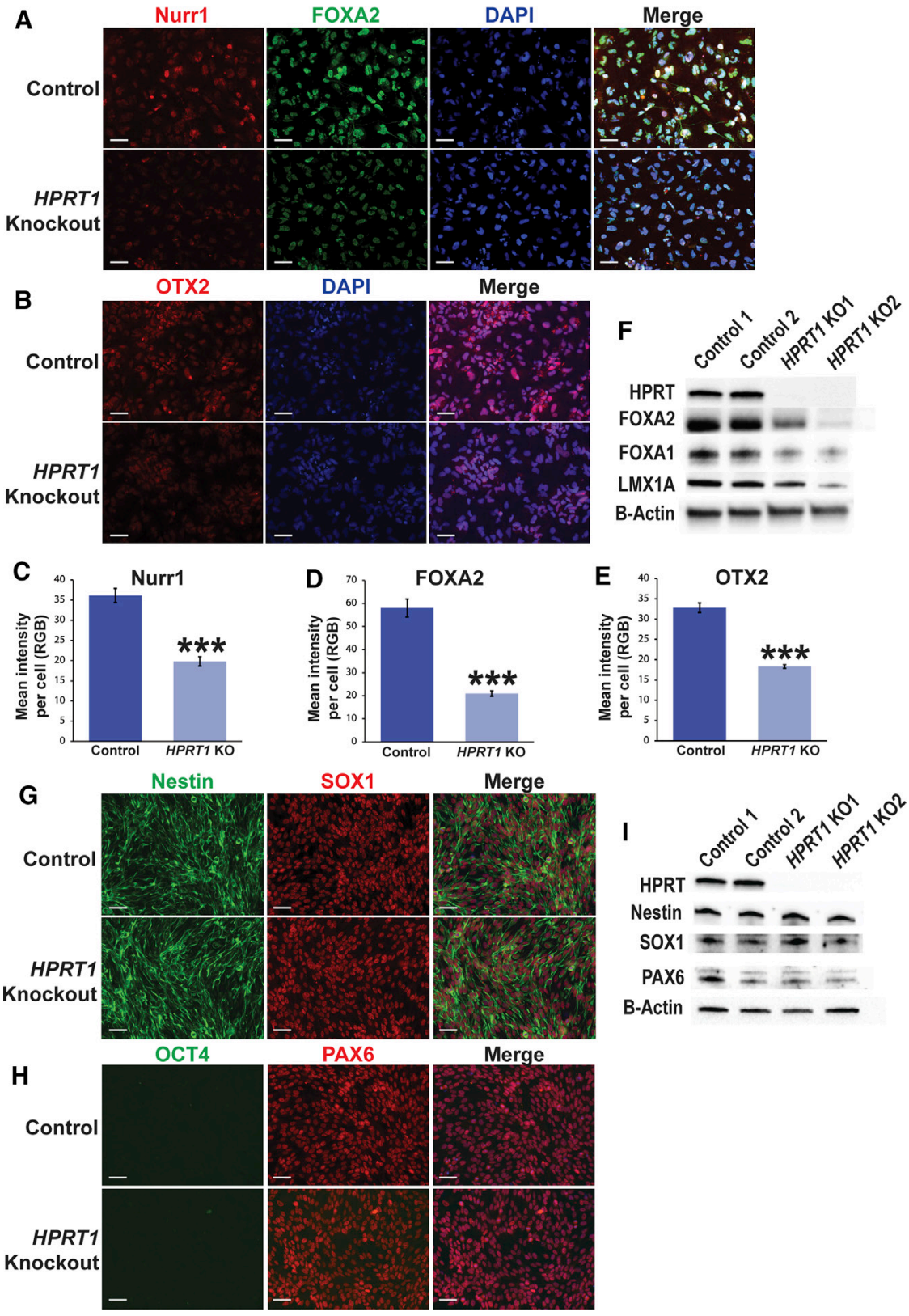
A
Nurr1
FOXA2
DAPI
Merge
Control
HPRT1 Knockout
B
OTX2
DAPI
Merge
Control
HPRT1 Knockout
F
Control 1
Control 2
HPRT1 KO1
HPRT1 KO2
HPRT
FOXA2
FOXA1
LMX1A
B-Actin
C
Nurr1
Mean intensity per cell (RGB)
***
Control
HPRT1 KO
D
FOXA2
Mean intensity per cell (RGB)
***
Control
HPRT1 KO
E
OTX2
Mean intensity per cell (RGB)
***
Control
HPRT1 KO
G
Nestin
SOX1
Merge
Control
HPRT1 Knockout
I
Control 1
Control 2
HPRT1 KO1
HPRT1 KO2
HPRT
Nestin
SOX1
PAX6
B-Actin
H
OCT4
PAX6
Merge
Control
HPRT1 Knockout

Figure 1. *HPRT1* knockout reduces the intensity of cell-fate markers in committed midbrain dopaminergic neural progenitor cells

n = 2 independent iPSC-derived clones from one control individual, and 2 different KO editing events from the same individual throughout this figure. Replicates are different clones and independent analyses from the same cell line.

(A) ICC for dopaminergic markers Nurr1 (NR4A2) and FOXA2 in *HPRT1* KO and control DA NPCs. Scale bar represents 50 mm.

(B) ICC for dopaminergic marker OTX2 in *HPRT1* KO and control DA NPCs. Scale bar represents 50 mm.

(C) Mean signal intensity per cell area from Nurr1 ICC images, as measured in QuPath. Data are derived from four separate cell lines (two control and two KO from a single individual). Eight images were used per cell line. Significance is based on Student's t test (***$p < 0.001$).

(D) Mean signal intensity per cell area from FOXA2 ICC images, as measured in QuPath. Data are derived from four separate cell lines (two control and two KO from a single individual). Eight images were used per cell line. Significance is based on Student's t test (***$p < 0.001$).

(E) Mean signal intensity per cell area from OTX2 ICC images, as measured in QuPath. Data are derived from four separate cell lines (two control and two KO from a single individual). Eight images were used per cell line. Significance is based on Student's t test (***$p < 0.001$).

(F) Western blots for dopaminergic markers in *HPRT1* KO and control DA NPCs.

(G) ICC for Nestin and SOX1 in *HPRT1* KO and control CN NPCs. Scale bar represents 50 mm.

(H) ICC for OCT4 and PAX6 in *HPRT1* KO and control CN NPCs. Scale bar represents 50 mm.

(I) Western blots for cortical markers in *HPRT1* KO and control CN NPCs.

Figure 2

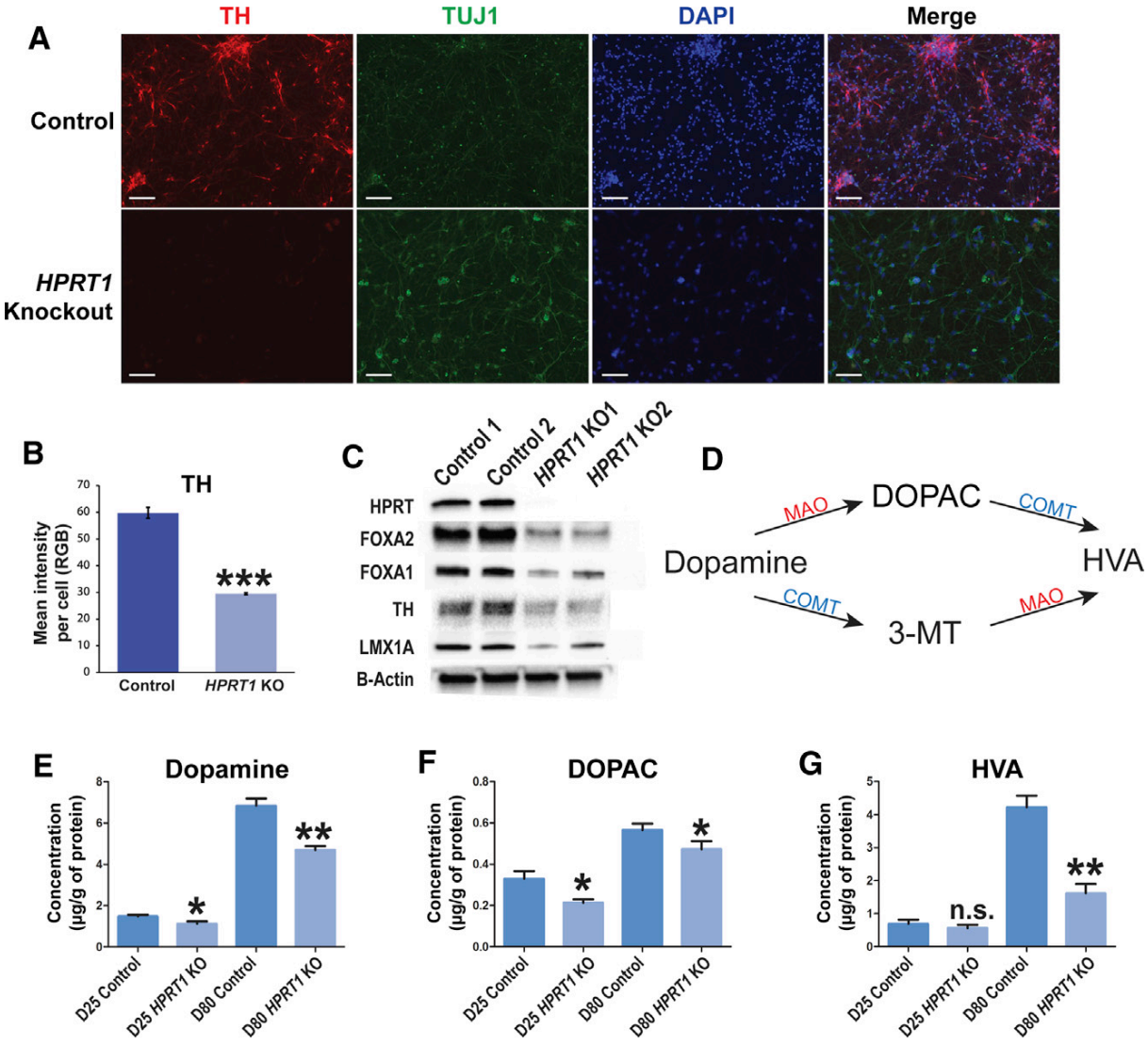
A
TH
TUJ1
DAPI
Merge
Control
HPRT1 Knockout
B
TH
Mean intensity per cell (RGB)
***
Control
HPRT1 KO
C
Control 1
Control 2
HPRT1 KO1
HPRT1 KO2
HPRT
FOXA2
FOXA1
TH
LMX1A
B-Actin
D
MAO
DOPAC
COMT
Dopamine
HVA
COMT
3-MT
MAO
E
Dopamine
Concentration (µg/g of protein)
D25 Control
D25 HPRT1 KO
D80 Control
D80 HPRT1 KO
F
DOPAC
G
HVA
n.s.

Figure 2. *HPRT1* knockout leads to loss of cell identity and dopaminergic metabolites in dopaminergic neurons

n = 2 independent iPSC-derived clones from one control individual, and 2 different KO editing events from the same individual throughout this figure. Replicates are different clones and independent analyses from the same cell line.

(A) ICC for the dopaminergic marker TH in *HPRT1* KO and control DA neurons. Scale bar represents 50 mm.

(B) Mean signal intensity per cell area from TH ICC images, as measured in QuPath. Data are derived from four separate cell lines (two control and two KO from a single individual). Eight images were used per cell line. Significance is based on Student's t test (***$p < 0.001$).

(C) Western blots for dopaminergic markers in *HPRT1* KO and control DA neurons.

(D) Diagram of dopamine metabolism.

(E–G) HPLC measurements of dopamine, 3,4-dihydroxyphenylacetic acid (DOPAC), and homovanillic acid (HVA) in day 25 and day 80 *HPRT1* KO and control neurons. Significance is based on Student's t test comparing *HPRT1* KO to control cells at matched time points (*$p < 0.05$, **$p < 0.01$). n = 4 separate cell lines with four replicates used per cell line for 16 total data points.

Figure 3

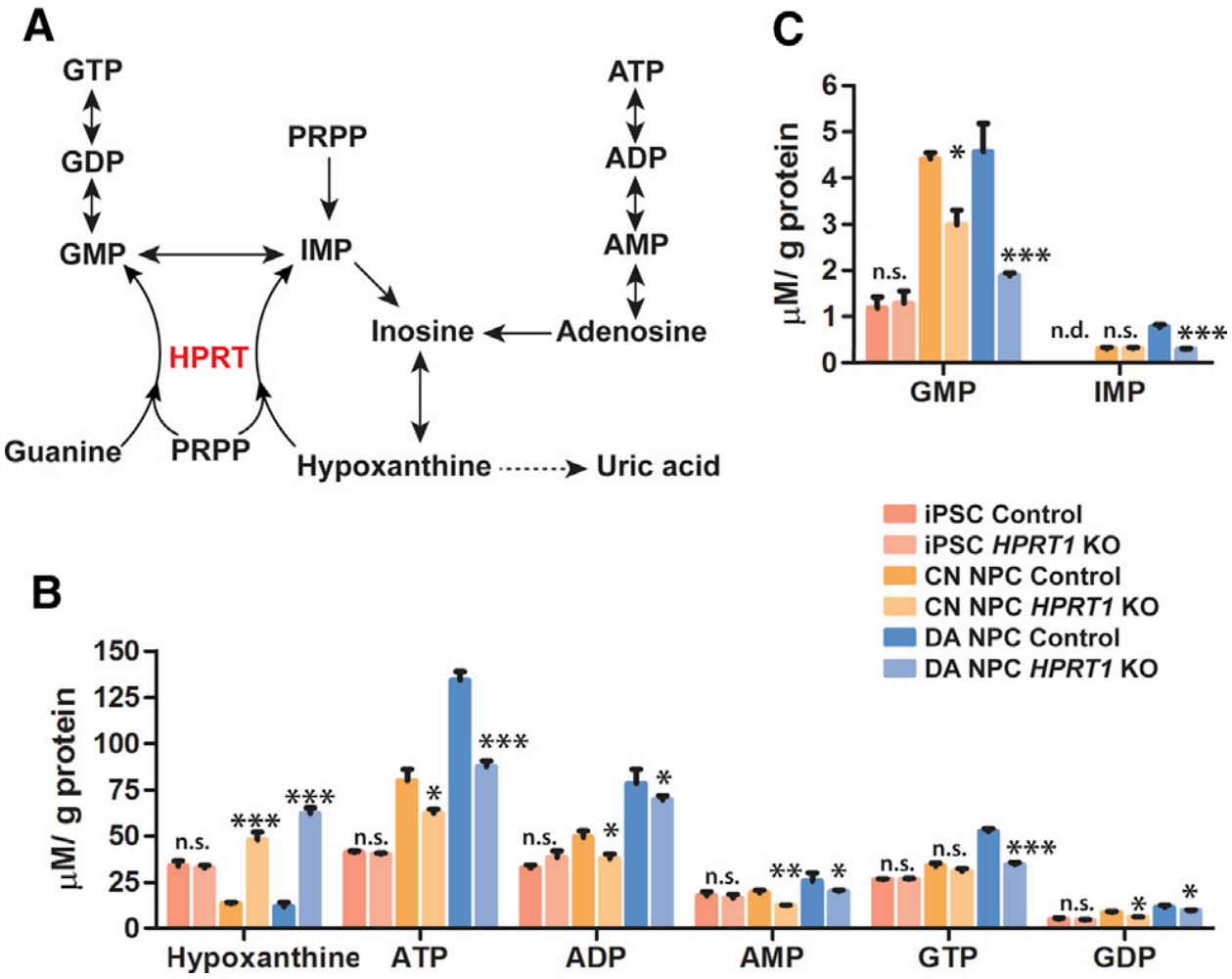
A
GTP
GDP
GMP
PRPP
IMP
ATP
ADP
AMP
Inosine
Adenosine
HPRT
Guanine
PRPP
Hypoxanthine
Uric acid
C
µM/ g protein
n.s.
*
***
n.d.
n.s.
***
GMP
IMP
B
iPSC Control
iPSC HPRT1 KO
CN NPC Control
CN NPC HPRT1 KO
DA NPC Control
DA NPC HPRT1 KO
µM/ g protein
Hypoxanthine
ATP
ADP
AMP
GTP
GDP

Figure 3. *HPRT1* knockout depletes purine metabolites in midbrain and cortical neural progenitor cells

n = 2 independent iPSC-derived clones from one control individual, and 2 different KO editing events from the same individual throughout this figure. Replicates are different clones and independent analyses from the same cell line.

(A) Diagram of purine metabolism.

(B and C) HPLC measurements for purine metabolites in iPSCs, cortical NPCs, and dopaminergic NPCs in *HPRT1* KO and isogenic controls. Significance is based on Student's t test comparing *HPRT1* KO to control cell within each cell type. Six to eight replicates were used for each cell line (*$p < 0.05$, **$p < 0.01$, ***$p < 0.001$; n.s., not significant; n.d., not detected).

Figure 4

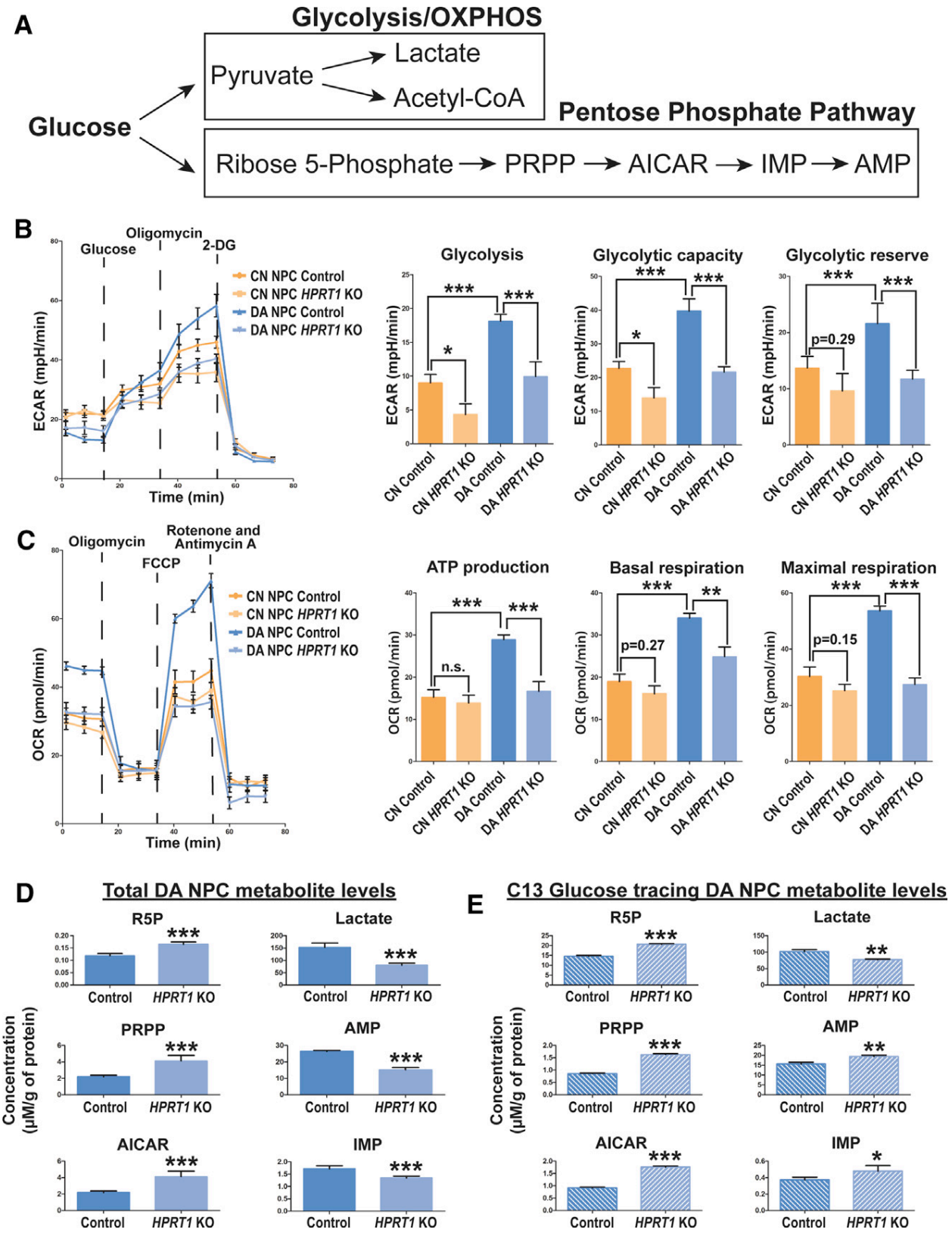
A
Glycolysis/OXPHOS
Pyruvate
Lactate
Acetyl-CoA
Glucose
Pentose Phosphate Pathway
Ribose 5-Phosphate → PRPP → AICAR → IMP → AMP
B
Oligomycin
Glucose
2-DG
ECAR (mpH/min)
Time (min)
CN NPC Control
CN NPC HPRT1 KO
DA NPC Control
DA NPC HPRT1 KO
Glycolysis
Glycolytic capacity
Glycolytic reserve
p=0.29
C
Oligomycin
Rotenone and Antimycin A
FCCP
OCR (pmol/min)
Time (min)
ATP production
Basal respiration
Maximal respiration
n.s.
p=0.27
p=0.15
CN Control
CN HPRT1 KO
DA Control
DA HPRT1 KO
D
Total DA NPC metabolite levels
R5P
Lactate
PRPP
AMP
AICAR
IMP
Concentration (μM/g of protein)
Control
HPRT1 KO
E
C13 Glucose tracing DA NPC metabolite levels

Figure 4. Differential effects of *HPRT1* knockout on glycolysis, oxidative phosphorylation, and glucose utilization in midbrain and cortical NPCs

n = 2 independent iPSC-derived clones from one control individual, and 2 different KO editing events from the same individual throughout this figure, except where indicated. Replicates are different clones and independent analyses from the same cell line.

(A) Diagram showing possible destinations of glucose of metabolites.

(B) Glycolysis measurements made via a Seahorse measurement of extracellular acidification. Graphs on the right summarize the data displayed on the left. Significance is based on a one-way ANOVA (*$p < 0.05$, ***$p < 0.001$). n = 4 separate cell lines with at least three or four replicates per line. 2-DG, 2-deoxyglucose.

(C) Oxidative phosphorylation measurements made via a Seahorse measurement of oxygen consumption. Bar graphs on the right summarize the data displayed on the left. Significance is based on a one-way ANOVA (**$p < 0.01$, ***$p < 0.001$). n = 4 separate cell lines with three or four replicates per line. FCCP, carbonyl cyanide 4-(trifluoromethoxy) phenylhydrazone.

(D) HPLC measurements of metabolites in the PPP and glycolytic pathways measured in *HPRT1* KO and isogenic control DA NPCs. n = 2 cell lines (one control and one KO) and three or four replicates per line. Significance is based on Student's t test (***$p < 0.001$).

(E) C13 levels of metabolites in *HPRT1* KO and isogenic control DA NPCs 2 h after being exposed to C13 glucose. n = 2 cell lines (one control and one KO) with three or four replicates per line. Significance is based on Student's t test (*$p < 0.05$, **$p < 0.01$, ***$p < 0.001$).

Figure 5

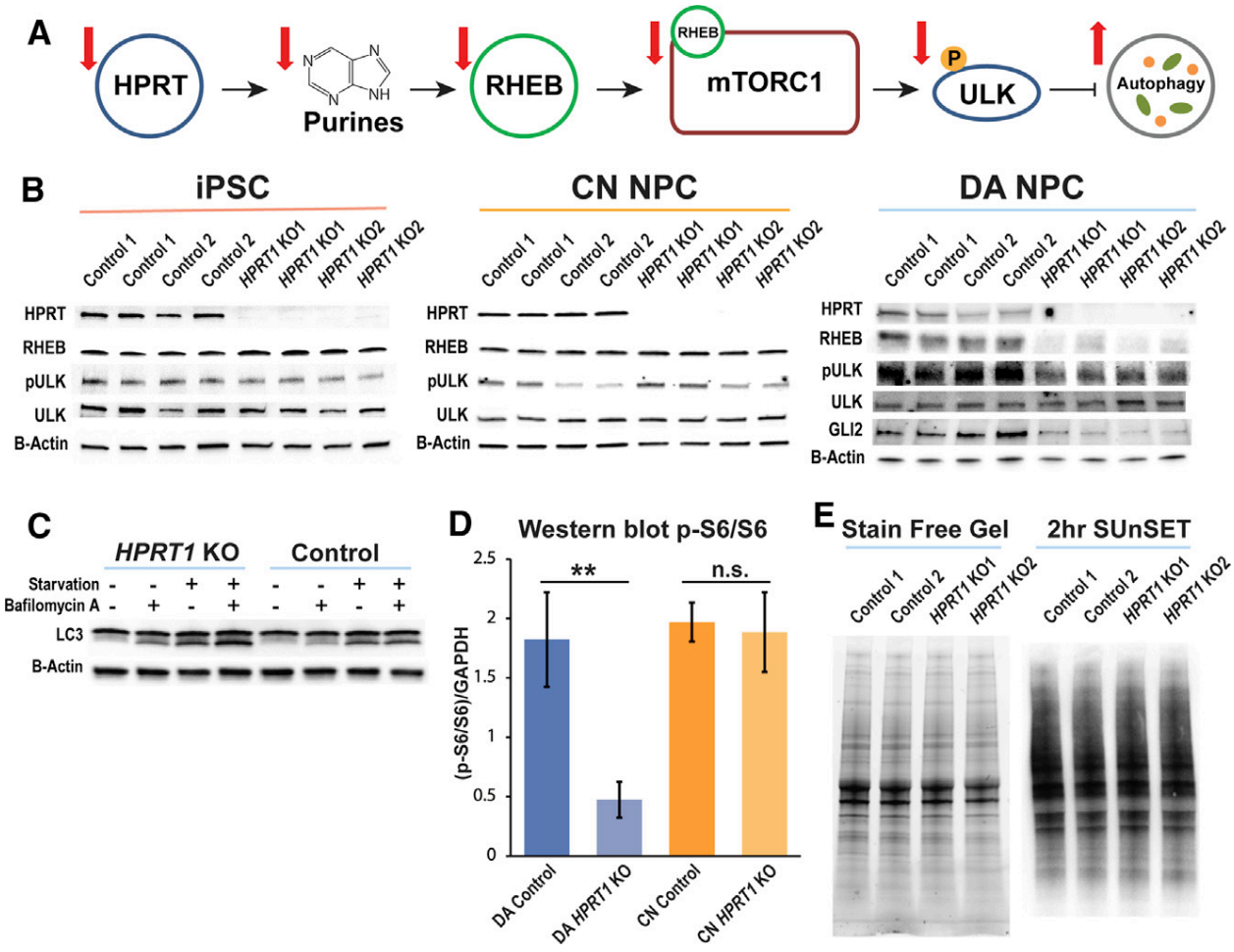
A
HPRT
Purines
RHEB
RHEB
mTORC1
P
ULK
Autophagy
B
iPSC
CN NPC
DA NPC
Control 1
Control 1
Control 2
Control 2
HPRT1 KO1
HPRT1 KO1
HPRT1 KO2
HPRT1 KO2
HPRT
RHEB
pULK
ULK
GLI2
B-Actin
C
HPRT1 KO
Control
Starvation
Bafilomycin A
LC3
B-Actin
D
Western blot p-S6/S6
(p-S6/S6)/GAPDH
2.5
2
1.5
1
0.5
0
**
n.s.
DA Control
DA HPRT1 KO
CN Control
CN HPRT1 KO
E
Stain Free Gel
2hr SUnSET
Control 1
Control 2
HPRT1 KO1
HPRT1 KO2

Figure 5. *HPRT1* knockout leads to decreased mTORC1 activity in midbrain NPCs, but not in cortical NPCs or iPSCs

n = 2 independent iPSC-derived clones from one control individual, and 2 different KO editing events from the same individual hroughout this figure. Replicates are different clones and independent analyses from the same cell line.

(A) Diagram illustrating how a decrease in HPRT activity relates to mTORC1 activity and autophagy.

(B) Western blots showing markers of mTORC1 activity in *HPRT1* KO and isogenic control iPSCs, CN NPCs, and DA NPCs. Two replicates per cell line.

(C) Western blot of LC3-I and LC3-II levels in control and isogenic *HPRT1* KO DA NPCs when exposed to 8 h of serum starvation and/or 10 nM bafilomycin A. One replicate per cell line.

(D) Western blot quantification for the ratio of p240/244-S6 to total S6 normalized to GAPDH for blots shown in Figure S4D. Three replicates per cell line (**$p < 0.01$).

(E) Stain-Free gel and SUnSET blot of *HPRT1* KO and isogenic control DA NPCs following 2 h of exposure to 10 mM puromycin. One replicate per cell line.

Figure 6

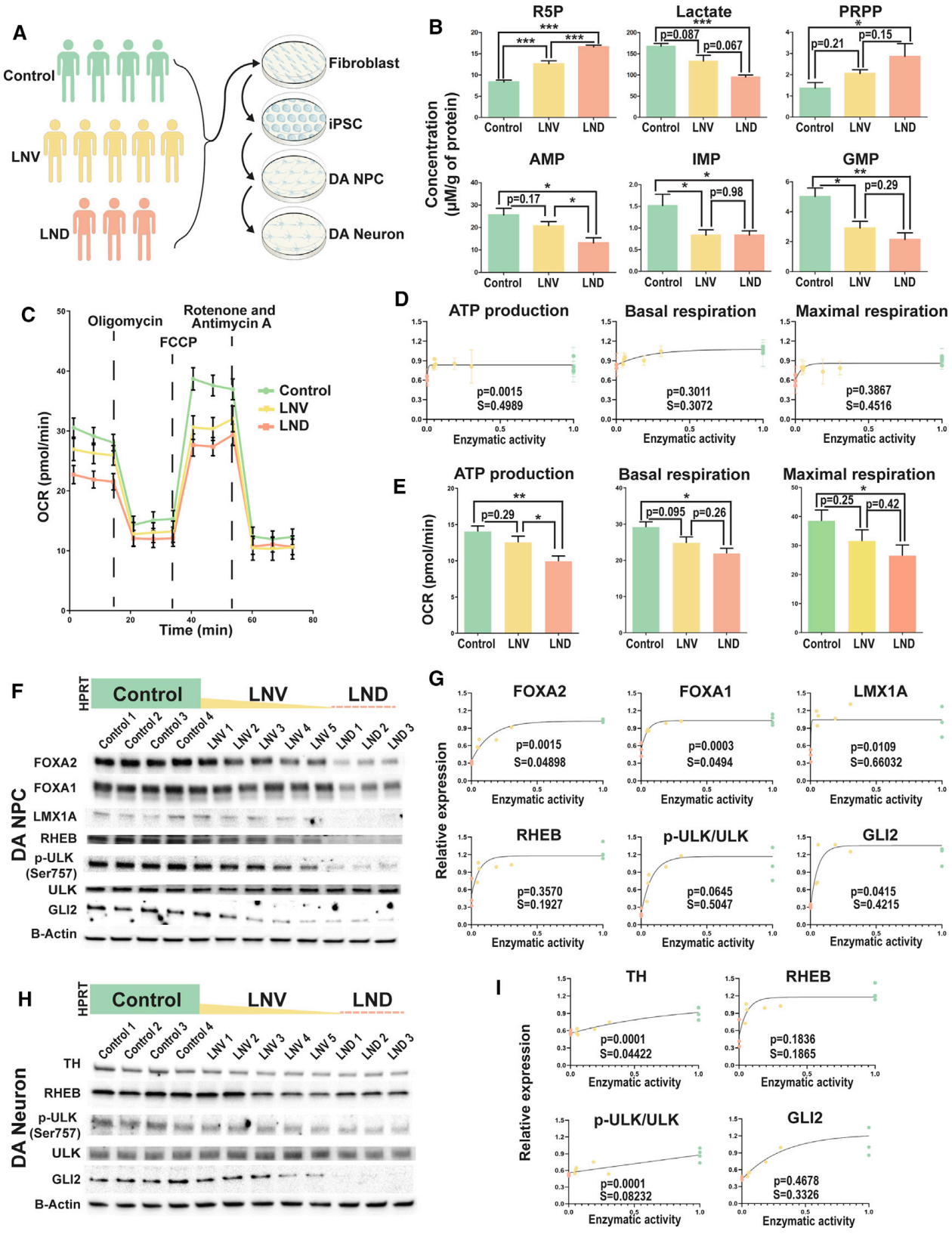
A
Control
LNV
LND
Fibroblast
iPSC
DA NPC
DA Neuron
B
R5P
Lactate
PRPP
AMP
IMP
GMP
Concentration (μM/g of protein)
Control
LNV
LND
p=0.087
p=0.067
p=0.21
p=0.15
p=0.17
p=0.98
p=0.29
C
Oligomycin
FCCP
Rotenone and Antimycin A
OCR (pmol/min)
Time (min)
D
ATP production
Basal respiration
Maximal respiration
p=0.0015
S=0.4989
p=0.3011
S=0.3072
p=0.3867
S=0.4516
Enzymatic activity
E
ATP production
Basal respiration
Maximal respiration
p=0.29
p=0.095
p=0.26
p=0.25
p=0.42
F
HPRT
Control
LNV
LND
Control 1
Control 2
Control 3
Control 4
LNV 1
LNV 2
LNV 3
LNV 4
LNV 5
LND 1
LND 2
LND 3
DA NPC
FOXA2
FOXA1
LMX1A
RHEB
p-ULK (Ser757)
ULK
GLI2
B-Actin
G
FOXA2
FOXA1
LMX1A
RHEB
p-ULK/ULK
GLI2
Relative expression
p=0.0015
S=0.04898
p=0.0003
S=0.0494
p=0.0109
S=0.66032
p=0.3570
S=0.1927
p=0.0645
S=0.5047
p=0.0415
S=0.4215
H
DA Neuron
TH
RHEB
p-ULK (Ser757)
ULK
GLI2
B-Actin
I
TH
RHEB
p-ULK/ULK
GLI2
p=0.0001
S=0.04422
p=0.1836
S=0.1865
p=0.0001
S=0.08232
p=0.4678
S=0.3326

Figure 6. LNV and LND cases reveal significant relationships between enzyme activity, OXPHOS potential, and dopaminergic marker expression in NPCs and neurons

All data are derived from four controls, five LNV subjects, and three LND subjects throughout this figure (n = 12 cell lines from 12 different people).

(A) Diagram illustrating the process of generating dopaminergic cells from four control, five LNV, and three LND subjects.

(B) HPLC measurements of metabolites from the patient cohort. Significance is based on Student's t test comparing LND and LNV patient cohorts to controls (*$p < 0.05$, **$p < 0.01$, ***$p < 0.001$). Three or four replicates per cell line.

(C) Oxidative phosphorylation measurements made via Seahorse for control, LND, and LNV dopaminergic NPC lines. Oxygen consumption rate was measured as the drugs indicated on the dashed lines were applied in succession over 12.5 min intervals. Three or four replicates per cell line.

(D) Scatterplot showing the relationship between HPRT activity in DA NPCs and the level of ATP production, basal respiration, and maximal respiration. Parameters were calculated using the data displayed in (C) and color coded based on patient cohort. Curves were generated based on a line of best fit based on an equation for one-phase decay. The p values represent relative likelihood of a one-phase exponential decay versus a linear relationship, calculated using the Akaike information criterion.

(E) Bar graphs summarizing key parameters from the OXPHOS data displayed in (D) by patient cohort. Significance is based on Student's t test comparing LND and LNV patient cohorts to controls (*$p < 0.05$, **$p < 0.01$).

(F) Western blot of control, LNV, and LND patient dopaminergic NPCs probed for dopaminergic and mTORC1 activity markers. All cell lines were lysed 24 ± 1 h after last medium exchange.

(G) Non-linear regression of protein expression data shown in (E). Curves were generated based on a line of best fit based on an equation for one-phase decay. The p values represent relative likelihood of a one-phase exponential decay versus a linear relationship, calculated using the Akaike information criterion.

(H) Western blot of control, LNV, and LND patient dopaminergic D15 neurons probed for dopaminergic and mTORC1 activity markers.

(I) Non-linear regression of protein expression data shown in (H). Curves were generated based on a line of best fit based on an equation for one-phase decay, for GLI2 and RHEB, and a linear line of best fit for TH and pULK/total ULK. The p values represent relative likelihood of a one-phase exponential decay versus a linear relationship, calculated using the Akaike information criterion.

REFERENCES

Bell, S., Kolobova, I., Crapper, L., and Ernst, C. (2016). Lesch-Nyhan syndrome: models, theories, and therapies. Mol. Syndromol. 7, 302–311. https://doi.org/10.1159/000449296.

Bell, S., Hettige, N.C., Silveira, H., Peng, H., Wu, H., Jefri, M., Antonyan, L., Zhang, Y., Zhang, X., and Ernst, C. (2019). Differentiation of human induced pluripotent stem cells (iPSCs) into an effective model of forebrain neural progenitor cells and mature neurons. Bio Protoc. 9. https://doi.org/10.21769/bioprotoc.3188.

Biever, A., Valjent, E., and Puighermanal, E. (2015). Ribosomal protein S6 phosphorylation in the nervous system: from regulation to function. Front. Mol. Neurosci. 8, 75. https://doi.org/10.3389/fnmol.2015.00075.

Bitler, C.M., and Howard, B.D. (1986). Dopamine metabolism in hypoxanthine-guanine phosphoribosyltransferase-deficient variants of PC12 cells. J. Neurochem. 47, 107–112. https://doi.org/10.1111/j.1471-4159.1986.tb02837.x.

Bozadjieva, N., Blandino-Rosano, M., Chase, J., Dai, X.Q., Cummings, K., Gimeno, J., Dean, D., Powers, A.C., Gittes, G.K., Ru¨egg, M.A., et al. (2017). Loss of mTORC1 signaling alters pancreatic a cell mass and impairs glucagon secretion. J. Clin. Invest. 127, 4379–4393. https://doi.org/10.1172/JCI90004.

Chan, E.Y., Longatti, A., McKnight, N.C., and Tooze, S.A. (2009). 'Kinase-Inactivated ULK proteins inhibit autophagy via their conserved C-terminal domains using an atg13-independent mechanism. Mol. Cell Biol. 29, 157–171. https://doi.org/10.1128/mcb.01082-08.

Cork, G.K., Thompson, J., and Slawson, C. (2018). Real talk: the inter-play between the mTOR, AMPK, and hexosamine biosynthetic pathways in cell signaling. Front. Endocrinol. 9, 522. https://doi.org/10.3389/fendo.2018.00522.

Costa, M.R.C., Edelstein, S.B., Castiglione, C.M., Chao, H., and Breakefield, X.O. (1980). Properties of monoamine oxidase in control and Lesch-Nyhan fibroblasts. Biochem. Genet. 18, 577–590. https://doi.org/10.1007/BF00484403.

Cox, R.P., Krauss, M.R., Balis, M.E., and Dancis, J. (1970). 'Evidence for transfer of enzyme product as the basis of metabolic cooperation between tissue culture fibroblasts of Lesch-Nyhan disease and normal cells. Proc. Natl. Acad. Sci. U S A 67, 1573–1579. https://doi.org/10.1073/pnas.67.3.1573.

Edelstein, S.B., Castiglione, C.M., and Breakfield, X.O. (1978). Monoamine oxidase activity in normal and lesch-nyhan fibroblasts. J. Neurochem. 31, 1247–1254. https://doi.org/10.1111/j.1471-4159.1978.tb06249.x.

Egami, K., Yitta, S., Kasim, S., Lewers, J.C., Roberts, R.C., Lehar, M., and Jinnah, H.A. (2007). Basal ganglia dopamine loss due to defect in purine recycling. Neurobiol. Dis. 26, 396–407. https://doi.org/10.1016/j.nbd.2007.01.010.

Emmanuel, N., Ragunathan, S., Shan, Q.,Wang, F., Giannakou, A., Huser, N., Jin, G., Myers, J., Abraham, R.T., and Unsal-Kacmaz, K. (2017). Purine nucleotide availability regulates mTORC1 activity through the rheb GTPase. Cell Rep. 19, 2665–2680. https://doi.org/10.1016/j.celrep.2017.05.043.

Ernst, M., Zametkin, A.J., Matochik, J.A., Pascualvaca, D., Jons, P.H., Hardy, K., Hankerson, J.G., Doudet, D.J., and Cohen, R.M. (1996). 'Presynaptic dopaminergic deficits in lesch–nyhan disease'. N. Engl. J. Med. 334, 1568–1572. https://doi.org/10.1056/NEJM199606133342403.

Ferri, A.L., Lin, W., Mavromatakis, Y.E., Wang, J.C., Sasaki, H., Whitsett, J.A., and Ang, S.L. (2007). Foxa1 and Foxa2 regulate multiple phases of midbrain dopaminergic neuron development in a dosage-dependent manner. Development 134, 2761–2769. https://doi.org/10.1242/dev.000141.

Fu, R., Sutcliffe, D., Zhao, H., Huang, X., Schretlen, D.J., Benkovic, S., and Jinnah, H.A. (2015). Clinical severity in lesch-Nyhan disease: the role of residual enzyme and compensatory pathways. Mol. Genet. Metab. 114, 55–61. https://doi.org/10.1016/j.ymgme.2014.11.001.

Gao, L., Zhou,W., Symmes, B., and Freed, C.R. (2016). Re-cloning the N27 dopamine cell line to improve a cell culture model of Parkinson's disease. PLoS One 11, e0160847. https://doi.org/10.1371/journal.pone.0160847.

Gao, N., Le Lay, J., Qin, W., Doliba, N., Schug, J., Fox, A.J., Smirnova, O., Matschinsky, F.M., and Kaestner, K.H. (2010). Foxa1 and Foxa2 maintain the metabolic and secretory features of the mature beta-cell. Mol. Endocrinol. 24, 1594–1604. https://doi.org/10.1210/me.2009-0513.

Garcia, D., and Shaw, R.J. (2017). AMPK: mechanisms of cellular energy sensing and restoration of metabolic balance. Mol. Cell 66, 789–800. https://doi.org/10.1016/j.molcel.2017.05.032.

Garza-Lombo´ , C., and Gonsebatt, M.E. (2016). Mammalian target of rapamycin: its role in early neural development and in adult and aged brain function. Front. Cell. Neurosci. 10, 157. https://doi.org/10.3389/fncel.2016.00157.

Go¨ttle, M., Prudente, C.N., Fu, R., Sutcliffe, D., Pang, H., Cooper, D., Veledar, E., Glass, J.D., Gearing, M., Visser, J.E., and Jinnah, H.A. (2014). Loss of dopamine phenotype among midbrain neurons in Lesch-Nyhan disease. Ann. Neurol. 76, 95–107. https://doi.org/10.1002/ana.24191.

Gwinn, D.M., Shackelford, D.B., Egan, D.F., Mihaylova, M.M., Mery, A., Vasquez, D.S., Turk, B.E., and Shaw, R.J. (2008). AMPK phosphorylation of raptor mediates a metabolic checkpoint. Mol. Cell 30, 214–226. https://doi.org/10.1016/j.molcel.2008.03.003.

Heddad Masson, M., Poisson, C., Gue´rardel, A., Mamin, A., Philippe, J., and Gosmain, Y. (2014). Foxa1 and Foxa2 regulate a-cell differentiation, glucagon biosynthesis, and secretion. Endocrinology 155, 3781–3792. https://doi.org/10.1210/en.2013-1843.

Hoxhaj, G., Hughes-Hallett, J., Timson, R.C., Ilagan, E., Yuan, M., Asara, J.M., Ben-Sahra, I., and Manning, B.D. (2017). The mTORC1 signaling network senses changes in cellular purine nucleotide levels. Cell Rep. 21, 1331–1346. https://doi.org/10.1016/j.celrep.2017.10.029.

Hynes, M., Porter, J.A., Chiang, C., Chang, D., Tessier-Lavigne, M., Beachy, P.A., and Rosenthal, A. (1995). Induction of midbrain dopaminergic neurons by Sonic hedgehog. Neuron 15, 35–44. https://doi.org/10.1016/0896-6273(95)90062-4.

Jefri, M., Bell, S., Peng, H., Hettige, N., Maussion, G., Soubannier, V., Wu, H., Silveira, H., Theroux, J.F., Moquin, L., et al. (2020). 'Stimulation of L-type calcium channels increases tyrosine

hydroxylase and dopamine in ventral midbrain cells induced from somatic cells'. Stem Cells Transl. Med. 9, 18–0180. https://doi.org/10.1002/sctm.18-0180.

Jinnah, H.A., Visser, J.E., Harris, J.C., Verdu, A., Larovere, L., Ceballos-Picot, I., Gonzalez-Alegre, P., Neychev, V., Torres, R.J., Dulac, O., et al. (2006). 'Delineation of the motor disorder of Lesch–Nyhan disease'. Brain 129, 1201–1217. https://doi.org/10.1093/brain/awl056.

Jinnah, H.A. (2009). Lesch-Nyhan disease: from mechanism to model and back again. Dis. Models Mech., 116–121. https://doi.org/10.1242/dmm.002543.

Jinnah, H.A., Ceballos-Picot, I., Torres, R.J., Visser, J.E., Schretlen, D.J., Verdu, A., Laro´ vere, L.E., Chen, C.J., Cossu, A., Wu, C.H., et al. (2010). Attenuated variants of Lesch-Nyhan disease. Brain 133, 671–689. https://doi.org/10.1093/brain/awq013.

Ka, M., Condorelli, G., Woodgett, J.R., and Kim, W.Y. (2014). mTOR regulates brain morphogenesis by mediating GSK3 signaling. Development 141, 4076–4086. https://doi.org/10.1242/dev.108282.

La, H.M., Chan, A.L., Legrand, J.M.D., Rossello, F.J., Gangemi, C.G., Papa, A., Cheng, Q., Morand, E.F., and Hobbs, R.M. (2018). GILZ-dependent modulation of mTORC1 regulates spermatogonial maintenance. Development 145. https://doi.org/10.1242/dev.165324.

Lesch, M., and Nyhan,W.L. (1964). A familial disorder of uric acid metabolism and central nervous system function. Am. J. Med. 36, 561–570. https://doi.org/10.1016/0002-9343(64)90104-4.

Lewers, J.C., Ceballos-Picot, I., Shirley, T.L., Mockel, L., Egami, K., and Jinnah, H.A. (2008). Consequences of impaired purine recycling in dopaminergic neurons. Neuroscience 152, 761–772. https://doi.org/10.1016/j.neuroscience.2007.10.065.

Liesa, M., Palacı´n, M., and Zorzano, A. (2009). Mitochondrial dynamics in mammalian health and disease. Physiol. Rev. 89, 799–845. https://doi.org/10.1152/physrev.00030.2008.

Mamelak, M. (2018). Parkinson's disease, the dopaminergic neuron and gammahydroxybutyrate. Neurol. Ther. 7, 5–11. https://doi.org/10.1007/s40120-018-0091-2.

Meyuhas, O. (2015). Ribosomal protein S6 phosphorylation: four decades of research. Int. Rev. Cell Mol. Biol. 320, 41–73. https://doi.org/10.1016/bs.ircmb.2015.07.006.

Moffatt, B.A., and Ashihara, H. (2002). Purine and pyrimidine nucleotide synthesis and metabolism. Arabidopsis Book 1, e0018. https://doi.org/10.1199/tab.0018.

Murakami, M., Ichisaka, T., Maeda, M., Oshiro, N., Hara, K., Edenhofer, F., Kiyama, H., Yonezawa, K., and Yamanaka, S. (2004). mTOR is essential for growth and proliferation in early mouse embryos and embryonic stem cells. Mol. Cell Biol. 24, 6710–6718. https://doi.org/10.1128/MCB.24.15.6710-6718.2004.

Osborn, T., and Hallett, P.J. (2017). Seq-ing markers of midbrain dopamine neurons. Cell Stem Cell 20, 11–12. https://doi.org/10.1016/j.stem.2016.12.014.

Pacelli, C., Gigue`re, N., Bourque, M.J., Le´vesque, M., Slack, R.S., and Trudeau, L.E´ . (2015). Elevated mitochondrial bioenergetics and axonal arborization size are key contributors to the vulnerability of dopamine neurons. Curr. Biol. 25, 2349–2360. https://doi.org/10.1016/j.cub.2015.07.050.

Pampliega, O., and Cuervo, A.M. (2016). Autophagy and primary cilia: dual interplay. Curr. Opin. Cell Biol. 39, 1–7. https://doi.org/10.1016/j.ceb.2016.01.008.

Paul, G., Christophersen, N.S., Raymon, H., Kiaer, C., Smith, R., and Brundin, P. (2007). Tyrosine hydroxylase expression is unstable in a human immortalized mesencephalic cell line-Studies in vitro and after intracerebral grafting in vivo. Mol. Cell. Neurosci. 34, 390–399. https://doi.org/10.1016/j.mcn.2006.11.010.

Pedley, A.M., and Benkovic, S.J. (2017). A new view into the regulation of purine metabolism: the purinosome. Trends Biochem. Sci. 42, 141–154. https://doi.org/10.1016/j.tibs.2016.09.009.

Pristera`, A., Lin, W., Kaufmann, A.K., Brimblecombe, K.R., Threlfell, S., Dodson, P.D., Magill, P.J., Fernandes, C., Cragg, S.J., and Ang, S.L. (2015). Transcription factors FOXA1 and FOXA2 maintain dopaminergic neuronal properties and control feeding behavior in adult mice. Proc. Natl. Acad. Sci. U S A 112, E4929–E4938. https://doi.org/10.1073/pnas.1503911112.

Reily, C., Stewart, T.J., Renfrow, M.B., and Novak, J. (2019). Glycosylation in health and disease. Nat. Rev. Nephrol. 15, 346–366. https://doi.org/10.1038/s41581-019-0129-4.

Saucedo-Cardenas, O., Quintana-Hau, J.D., Le, W.D., Smidt, M.P., Cox, J.J., De Mayo, F., Burbach, J.P., and Conneely, O.M. (1998). Nurr1 is essential for the induction of the dopaminergic phenotype and the survival of ventral mesencephalic late dopaminergic precursor neurons. Proc. Natl. Acad. Sci. U S A 95, 4013–4018. https://doi.org/10.1073/pnas.95.7.4013.

Saxton, R.A., and Sabatini, D.M. (2017). mTOR signaling in growth, metabolism, and disease. Cell 168, 960–976. https://doi.org/10.1016/j.cell.2017.02.004.

Schmidt, E.K., Clavarino, G., Ceppi, M., and Pierre, P. (2009). SUn-SET, a nonradioactive method to monitor protein synthesis. Nat.Methods 6, 275–277. https://doi.org/10.1038/nmeth.1314.

Sidi, Y., and Mitchell, B.S. (1985). Z-nucleotide accumulation in erythrocytes from Lesch-Nyhan patients. J. Clin. Invest. 76, 2416–2419. https://doi.org/10.1172/JCI112255.

Sun, Y., Connors, K.E., and Yang, D.Q. (2007). AICAR induces phosphorylation of AMPK in an ATM-dependent, LKB1-independent manner. Mol. Cell. Biochem 306, 239–245. https://doi.org/10.1007/s11010-007-9575-6.

Sutcliffe, D.J., Dinasarapu, A.R., Visser, J.E., Hoed, J.D., Seifar, F., Joshi, P., Ceballos-Picot, I., Sardar, T., Hess, E.J., Sun, Y.V., et al. (2021). Induced pluripotent stem cells from subjects with Lesch-Nyhan disease. Sci. Rep. 11, 8523. https://doi.org/10.1038/s41598-021-87955-9.

Takahashi, K., Tanabe, K., Ohnuki, M., Narita, M., Ichisaka, T., Tomoda, K., and Yamanaka, S. (2007). Induction of pluripotent stem cells from adult human fibroblasts by defined factors. Cell 131, 861–872. https://doi.org/10.1016/j.cell.2007.11.019.

Wang, H.X., Shin, J., Wang, S., Gorentla, B., Lin, X., Gao, J., Qiu,Y.R., and Zhong, X.P. (2016). mTORC1 in thymic epithelial cells is critical for thymopoiesis, T-cell generation, and temporal control of gdT17 development and tcrg/d recombination. PLoS Biol. 14, e1002370. https://doi.org/10.1371/journal.pbio.1002370.

Watts, R.W., Spellacy, E., Gibbs, D.A., Allsop, J., McKeran, R.O., and Slavin, G.E. (1982). Clinical, post-mortem, biochemical and therapeutic observations on the lesch-nyhan syndrome with particular reference to the neurological manifestations. Q. J. Med. 51, 43–78. https://doi.org/10.1093/oxfordjournals.qjmed.a067707.

Wu, C.C., Hou, S., Orr, B.A., Kuo, B.R., Youn, Y.H., Ong, T., Roth, F., Eberhart, C.G., Robinson, G.W., Solecki, D.J., et al. (2017). mTORC1-Mediated inhibition of 4EBP1 is essential for hedgehog signaling-driven translation and medulloblastoma. Dev. Cell 43, 673–688.e5. https://doi.org/10.1016/j.devcel.2017.10.011.

Yan, B., Zhang, Z., Jin, D., Cai, C., Jia, C., Liu, W., Wang, T., Li, S., Zhang, H., Huang, B., et al. (2016). mTORC1 regulates PTHrP to coordinate chondrocyte growth, proliferation and differentiation. Nat. Commun. 7, 11151. https://doi.org/10.1038/ncomms11151.

Yanagiya, A., Suyama, E., Adachi, H., Svitkin, Y.V., Aza-Blanc, P., Imataka, H., Mikami, S., Martineau, Y., Ronai, Z.A., and Sonenberg, N. (2012). Translational homeostasis via the mRNA cap-binding protein, eIF4E. Mol. Cell 46, 847–858. https://doi.org/10.1016/j.molcel.2012.04.004.

Yeh, J., Zheng, S., and Howard, B.D. (1998). 'Impaired differentiation of HPRT-deficient dopaminergic neurons: a possible mechanism underlying neuronal dysfunction in Lesch-Nyhan syndrome'. J. Neurosci. Res. 53, 78–85. https://doi.org/10.1002/(SICI)1097-4547(19980701)53:1<78::AID-JNR8>3.0.CO;2-G.

Chapter 4: General Discussion

The findings presented in "Lesch-Nyhan disease causes impaired energy metabolism and reduced developmental potential in midbrain dopaminergic cells", published in Stem Cell Reports and reproduced as herein as Chapter 3, represent progress toward a complete mechanistic understanding of the link between mutations in *HPRT1* and the severe and consequential reduction of dopamine in the brains of individuals with Lesch-Nyhan disease.

The section titled "Objectives and Hypothesis" at the end of Chapter 1 outlined three central questions for the research to address:

4. *When in neurodevelopment, modelled in vitro, do cells with HPRT deficiency begin to show effects of loss of HPRT and which cell lineages are affected?*
5. *Is there a pre-existing property of those affected cell lineages that caused them to be vulnerable to HPRT deficiency when related neural cell lineages are not affected?*
6. *Concerning the cell lineages which do show effects of HPRT loss, what is occurring in those cells as a result of HPRT deficiency that could explain reduced dopamine in the brain?*

In response to the first question, ICC revealed that neither iPSC, CN NPC, nor CN neuron marker expression was affected by loss of HPRT. In contrast, DA NPC and DA neuron markers were expressed at significantly lower levels. This was in alignment with previous studies' observations of reduced dopamine output in the brains of patients with Lesch-Nyhan disease.

Addressing to the second question, experimentation revealed that control DA NPCs are more metabolically active than control CN NPCs, despite similar morphology. HPLC data indicated that control DA NPCs contained greater than 1.5 times the amount of ATP measured in CN NPC, with directionally similar findings seen for other purine metabolites. Seahorse data corroborated this,

with control DA NPC metrics of glycolysis and ATP production nearly double those of control CN NPC. This high baseline metabolic rate for normal DA NPCs indicates a greater need for energy and suggests a distinct vulnerability in the event of an energy crisis. This finding was a highlight of the research as it contradicts conventional thinking that the high metabolic rate seen in DA neurons is a result of highly arborized morphology and pacemaker activity (Pacelli et al. 2015).

In response to the third question, several effects of HPRT deficiency were seen in DA NPC that may contribute to impaired differentiation of DA neurons and therefore reduced dopamine output. HPLC revealed an increase in *de novo* purine synthesis. Western blot showed decreased mtTORC1 activation and a resulting increase in autophagy. Seahorse assays identified a reduction in measurements of glycolysis and oxidative phosphorylation.

The central hypothesis to this investigation — *that the dopaminergic lineage of cells in the developing brain is especially vulnerable to the loss of purine salvage caused by HPRT deficiency and as a result does not yield fully functional dopaminergic neurons* — was supported by the findings; however, there remains more to uncover in order to link the effects of HPRT deficiency and impaired differentiation of DA neurons.

There is a possibility that normal expression of DA markers and differentiation to functional DA neurons is impaired by the activation of a stem cell-like expression profile at the DA NPC stage. This stem-like expression profile may be activated by the unique effects of HPRT deficiency observed in DA NPCs, including increased *de novo* purine synthesis, increased autophagy, reduced mTORC1 activation, and reduced oxidative phosphorylation. The following paragraphs elaborate on the idea that the unique effects of HPRT deficiency observed in DA NPCs have the potential to

activate a stem-like expression profile with support from existing literature, and offers possible means of further investigating this possibility.

Though morphologically normal, HPRT-deficient DA NPCs did exhibit significantly less cell death than control DA NPCs, as measured by a TUNEL assay described in Chapter 2 and stated in Chapter 3. This reduction in observed cell death in cells lacking HPRT may suggest that the cells are in a more proliferative state than the control cells to which they are being compared. A key feature of stem cells is that they must be able to continually proliferate to be able to produce daughter cells. Differentiation away from the stem cell state is associated with reduced ability to proliferate(Liu et al. 2019). It is therefore possible that the reduced cell death in cells lacking HPRT is a behaviour indicative of a more stem-like state.

Another feature of proliferating cells compared to differentiated cells that is discussed in the literature is a preference for *de novo* purine synthesis over purine salvage (Villa et al. 2019) for the generation of purines. It may be that the increased *de novo* purine synthesis activity observed in DA NPC as a response to HPRT deficiency is supporting stem-like gene expression and activity in the cell. This may be via a mechanism that senses increased output or consumption of key metabolites and drives a stem-like gene expression profile in response. The promotion of stemness by *de novo* purine synthesis has already been shown in cancer cells (Lv et al. 2020). Similarly, iPSCs have been found to show higher levels of autophagy (Sotthibundhu et al. 2016), which is also a feature of HPRT-deficient DA NPCs presented as part of this thesis and described in Chapter 3. This possibility could be investigated control DA NPC by increasing *de novo* purine synthesis pharmacologically or perhaps by artificially increasing expression of genes involved in *de novo* purine synthesis. The hypothesis would be supported if the intervention were observed to increase stem-like behaviour or expression of genes associated with a stem-like state.

Moreover, it has been discovered that, in a key step during reprogramming to induced pluripotent stem cells, somatic cells go through a metabolic shift away from dependence on oxidative phosphorylation for energy production(Ishida et al. 2020). This behaviour of stem cells not to use oxidative phosphorylation for energy has been found to be essential for maintenance of stem cell properties and is referred to in studies of cancer as the Warburg effect (Ishida et al. 2020). In the case of Lesch-Nyhan disease, it may be that the loss of oxidative phosphorylation seen in HPRT-deficient DA NPCs as shown in this thesis may help drive a more stem-like gene expression profile. This may occur via a mechanism similar to the aforementioned metabolic shift away from dependence on oxidative phosphorylation for energy production that occurs during reprogramming by biologists of somatic cells to iPSCs.

Lastly, another possible mechanism by which HPRT deficiency could trigger a more stem-like expression profile may involve the reduction of mTORC1 activity in HPRT-deficient DA NPCs identified and discussed in Chapter 3. It may be that the reduction in mTORC1 activity triggered by the prolonged deficit of purines in cells lacking HPRT triggers the expression of key stem cell genes. It has already been shown in published literature that blockade of mTOR can drive an increase in the presence of the protein c-MYC (Shepherd et al. 2013), a highly-expressed, central regulatory protein in stem cells and one of the four Yamanaka stem cell factors (Takahashi et al. 2007). One could investigate this idea with control DA NPCs using rapamycin, an inhibitor of mTORC1. If the treatment of DA NPCs with rapamycin reduced mTORC1 activity and subsequently triggered the expression of stem cell genes, it would indicate that HPRT deficiency could trigger a more stem-like expression profile due to its effects on mTORC1 activation

Chapter 5: Conclusions and Future Directions

In conclusion, study of control, *HPRT1* knockout, and patient-derived cells, cultured as iPSC, NPC, and neuron, revealed consistent negative effects of HPRT deficiency on energy metabolism, mTORC1 activation, and developmental potential in the midbrain dopaminergic lineage. The extent of these effects is predicted by the magnitude of HPRT deficiency. The cell type specificity of the effect may result from the heightened energy state observed not only in DA neurons, but also in the DA NPCs which precede them. This knowledge may one day prove useful in the development of better treatments for those suffering the devastating consequences of Lesch-Nyhan disease.

Future research should focus on characterizing the expression patterns of stem cell markers in DA NPCs lacking functional HPRT. It would also be important to assess possible causal relationships between stem cell protein expression and the above findings, including elevated *de novo* purine synthesis, reduced oxidative phosphorylation, and impaired activation of mTORC1.

Chapter 6: References

American Psychiatric Association. 2013. *Diagnostic and Statistical Manual of Mental Disorders*. American Psychiatric Association. https://doi.org/10.1176/appi.books.9780890425596.

Anderson, LT, and M Ernst. 1994. "Self-Injury in Lesch-Nyhan Disease." *Journal of Autism and Developmental Disorders* 24 (1): 67–81. https://doi.org/10.1007/BF02172213.

Arim, Rubab G, Anton R Miller, Anne Guèvremont, Lucyna M Lach, Jamie C Brehaut, and Dafna E Kohen. 2017. "Children with Neurodevelopmental Disorders and Disabilities: A Population-Based Study of Healthcare Service Utilization Using Administrative Data." *Developmental Medicine & Child Neurology* 59 (12): 1284–90. https://doi.org/10.1111/dmcn.13557.

Ayano, Getinet. 2016. "Dopamine: Receptors, Functions, Synthesis, Pathways, Locations and Mental Disorders: Review of Literatures." *Journal of Mental Disorders and Treatment* 2 (2). https://doi.org/10.4172/2471-271X.1000120.

Bell, Scott, Vincent McCarty, Huashan Peng, Malvin Jefri, Nuwan Hettige, Lilit Antonyan, Liam Crapper, et al. 2021. "Lesch-Nyhan Disease Causes Impaired Energy Metabolism and Reduced Developmental Potential in Midbrain Dopaminergic Cells." *Stem Cell Reports* 16 (7): 1749–62. https://doi.org/10.1016/J.STEMCR.2021.06.003.

Bishop, Dorothy V. M. 2010. "Which Neurodevelopmental Disorders Get Researched and Why?" Edited by Rory Edward Morty. *PLoS ONE* 5 (11): e15112. https://doi.org/10.1371/journal.pone.0015112.

Bitler, Catherine M., and Bruce D. Howard. 1986. "Dopamine Metabolism in Hypoxanthine-Guanine Phosphoribosyltransferase-Deficient Variants of PC12 Cells." *Journal of Neurochemistry* 47 (1): 107–12. https://doi.org/10.1111/j.1471-4159.1986.tb02837.x.

Cooper, Oliver, Gunnar Hargus, Michela Deleidi, Alexandra Blak, Teresia Osborn, Elizabeth Marlow, Kristen Lee, et al. 2010. "Differentiation of Human ES and Parkinson's Disease IPS Cells into Ventral Midbrain Dopaminergic Neurons Requires a High Activity Form of SHH, FGF8a and Specific Regionalization by Retinoic Acid." *Molecular and Cellular Neuroscience* 45 (3): 258–66. https://doi.org/10.1016/J.MCN.2010.06.017.

Crawhall, J C, J F Henderson, and W N Kelley. 1972. "Diagnosis and Treatment of the Lesch-Nyhan Syndrome." *Pediatric Research* 6 (5): 504–13. https://doi.org/10.1203/00006450-197205000-00004.

Deon, Laura L., Miriam A. Kalichman, Cynthia L. Booth, Konstantin V. Slavin, and Deborah J. Gaebler-Spira. 2011. "Pallidal Deep-Brain Stimulation Associated With Complete Remission of Self-Injurious Behaviors in a Patient With Lesch-Nyhan Syndrome: A Case Report." *Http://Dx.Doi.Org/10.1177/0883073811415853* 27 (1): 117–20. https://doi.org/10.1177/0883073811415853.

Ducker, Gregory S., and Joshua D. Rabinowitz. 2017. "One-Carbon Metabolism in Health and Disease." *Cell Metabolism*. Cell Press. https://doi.org/10.1016/j.cmet.2016.08.009.

Emmanuel, Natasha, Shoba Ragunathan, Qin Shan, Fang Wang, Andreas Giannakou, Nanni Huser, Guixian Jin, Jeremy Myers, Robert T. Abraham, and Keziban Unsal-Kacmaz. 2017. "Purine Nucleotide Availability Regulates MTORC1 Activity through the Rheb GTPase." *Cell Reports* 19 (13): 2665–80. https://doi.org/10.1016/j.celrep.2017.05.043.

Ernst, Monique, Alan J. Zametkin, John A. Matochik, Daisy Pascualvaca, Peter H. Jons, Kristina Hardy, James G. Hankerson, Doris J. Doudet, and Robert M. Cohen. 1996. "Presynaptic Dopaminergic Deficits in Lesch–Nyhan Disease." *New England Journal of Medicine* 334 (24): 1568–72. https://doi.org/10.1056/NEJM199606133342403.

Foerster, Philippe, Marie Daclin, Shihavuddin Asm, Marion Faucourt, Alessandra Boletta, Auguste Genovesio, and Nathalie Spassky. 2017. "MTORC1 Signaling and Primary Cilia Are Required for Brain Ventricle Morphogenesis." *Development* 144 (2): 201–10. https://doi.org/10.1242/DEV.138271.

Gao, Lu, Wenbo Zhou, Breanna Symmes, and Curt R. Freed. 2016. "Re-Cloning the N27 Dopamine Cell Line to Improve a Cell Culture Model of Parkinson's Disease." *PLoS ONE* 11 (8). https://doi.org/10.1371/journal.pone.0160847.

Göttle, Martin, Cecilia N. Prudente, Rong Fu, Diane Sutcliffe, Hong Pang, Deborah Cooper, Emir Veledar, et al. 2014. "Loss of Dopamine Phenotype among Midbrain Neurons in Lesch-Nyhan Disease." *Annals of Neurology* 76 (1): 95–107. https://doi.org/10.1002/ana.24191.

Holczer, Marianna, Bence Hajdú, Tamás Lőrincz, András Szarka, Gábor Bánhegyi, and Orsolya Kapuy. 2019. "A Double Negative Feedback Loop between MTORC1 and AMPK Kinases Guarantees Precise Autophagy Induction upon Cellular Stress." *International Journal of Molecular Sciences* 20 (22). https://doi.org/10.3390/IJMS20225543.

Hoxhaj, Gerta, James Hughes-Hallett, Rebecca C. Timson, Erika Ilagan, Min Yuan, John M. Asara, Issam Ben-Sahra, and Brendan D. Manning. 2017. "The MTORC1 Signaling Network Senses Changes in Cellular Purine Nucleotide Levels." *Cell Reports* 21 (5): 1331–46. https://doi.org/10.1016/j.celrep.2017.10.029.

Ishida, Tomoaki, Shu Nakao, Tomoe Ueyama, Yukihiro Harada, and Teruhisa Kawamura. 2020. "Metabolic Remodeling during Somatic Cell Reprogramming to Induced Pluripotent Stem Cells: Involvement of Hypoxia-Inducible Factor 1." *Inflammation and Regeneration 2020 40:1* 40 (1): 1–8. https://doi.org/10.1186/S41232-020-00117-8.

Jinnah, H. A. 2009. “Lesch-Nyhan Disease: From Mechanism to Model and Back Again.” *DMM Disease Models and Mechanisms*. Company of Biologists. https://doi.org/10.1242/dmm.002543.

Jinnah, H. A., Laura De Gregorio, James C. Harris, William L. Nyhan, and J. Patrick O’Neill. 2000. “The Spectrum of Inherited Mutations Causing HPRT Deficiency: 75 New Cases and a Review of 196 Previously Reported Cases.” *Mutation Research/Reviews in Mutation Research* 463 (3): 309–26. https://doi.org/10.1016/S1383-5742(00)00052-1.

Jinnah, H. A., Jasper E. Visser, James C. Harris, Alfonso Verdu, Laura Larovere, Irene Ceballos-Picot, Pedro Gonzalez-Alegre, et al. 2006. “Delineation of the Motor Disorder of Lesch–Nyhan Disease.” *Brain* 129 (5): 1201–17. https://doi.org/10.1093/brain/awl056.

KG, Lloyd, Hornykiewicz O, Davidson L, Shannak K, Farley I, Goldstein M, Shibuya M, Kelley WN, and Fox IH. 1981. “Biochemical Evidence of Dysfunction of Brain Neurotransmitters in the Lesch-Nyhan Syndrome.” *The New England Journal of Medicine* 305 (19): 1106–11. https://doi.org/10.1056/NEJM198111053051902.

Kuehn, Michael R., Allan Bradley, Elizabeth J. Robertson, and Martin J. Evans. 1987. “A Potential Animal Model for Lesch-Nyhan Syndrome through Introduction of HPRT Mutations into Mice.” *Nature* 326 (6110): 295–98. https://doi.org/10.1038/326295a0.

Liu, Lijun, Wojciech Michowski, Aleksandra Kolodziejczyk, and Piotr Sicinski. 2019. “The Cell Cycle in Stem Cell Proliferation, Pluripotency and Differentiation.” *Nature Cell Biology* 21 (9): 1060–67. https://doi.org/10.1038/s41556-019-0384-4.

Lv, Yajing, Xiaoshuang Wang, Xiaoyu Li, Guangwei Xu, Yuting Bai, Jiayi Wu, Yongjun Piao, Yi Shi, Rong Xiang, and Longlong Wang. 2020. “Nucleotide de Novo Synthesis Increases Breast Cancer Stemness and Metastasis via CGMP-PKG-MAPK Signaling Pathway.”

PLOS Biology 18 (11): e3000872. https://doi.org/10.1371/JOURNAL.PBIO.3000872.

Murrell, G. A. C., and W. G. Rapeport. 2012. "Clinical Pharmacokinetics of Allopurinol." *Clinical Pharmacokinetics 1986 11:5* 11 (5): 343–53. https://doi.org/10.2165/00003088-198611050-00001.

Nguyen, Khue Vu, Robert K. Naviaux, and William L. Nyhan. 2017. "Novel Mutation in the Human HPRT1 Gene and the Lesch-Nyhan Disease." *Https://Doi.Org/10.1080/15257770.2017.1395037* 36 (11): 704–11. https://doi.org/10.1080/15257770.2017.1395037.

Nyhan, W. L. 1997. "The Recognition of Lesch-Nyhan Syndrome as an Inborn Error of Purine Metabolism." *Journal of Inherited Metabolic Disease 1997 20:2* 20 (2): 171–78. https://doi.org/10.1023/A:1005348504512.

Pacelli, Consiglia, Nicolas Giguère, Marie Josée Bourque, Martin Lévesque, Ruth S. Slack, and Louis Éric Trudeau. 2015. "Elevated Mitochondrial Bioenergetics and Axonal Arborization Size Are Key Contributors to the Vulnerability of Dopamine Neurons." *Current Biology* 25 (18): 2349–60. https://doi.org/10.1016/j.cub.2015.07.050.

Park, Sang Min, Hee Jin Jang, and Jeong Ho Lee. 2019. "Roles of Primary Cilia in the Developing Brain." *Frontiers in Cellular Neuroscience* 0 (May): 218. https://doi.org/10.3389/FNCEL.2019.00218.

Paul, Gesine, Nicolaj S. Christophersen, Heather Raymon, Caroline Kiaer, Ruben Smith, and Patrik Brundin. 2007. "Tyrosine Hydroxylase Expression Is Unstable in a Human Immortalized Mesencephalic Cell Line-Studies in Vitro and after Intracerebral Grafting in Vivo." *Molecular and Cellular Neuroscience* 34 (3): 390–99. https://doi.org/10.1016/j.mcn.2006.11.010.

Preston, Richard. 2007. “An Error in the Code.” *The New Yorker*, August 2007. https://www.newyorker.com/magazine/2007/08/13/an-error-in-the-code.

Sampat, Radhika, Rong Fu, Laura E. Larovere, Rosa J. Torres, Irene Ceballos-Picot, Michel Fischbach, Raquel de Kremer, David J. Schretlen, Juan Garcia Puig, and H. A. Jinnah. 2011. “Mechanisms for Phenotypic Variation in Lesch–Nyhan Disease and Its Variants.” *Human Genetics* 129 (1): 71. https://doi.org/10.1007/S00439-010-0901-9.

Seegmiller, J. Edwin, Frederick M. Rosenbloom, and William N. Kelley. 1967. “Enzyme Defect Associated with a Sex-Linked Human Neurological Disorder and Excessive Purine Synthesis.” *Science* 155 (3770): 1682–84. https://doi.org/10.1126/science.155.3770.1682.

Shepherd, C., L. Banerjee, C. W. Cheung, M. R. Mansour, S. Jenkinson, R. E. Gale, and A. Khwaja. 2013. “PI3K/MTOR Inhibition Upregulates NOTCH-MYC Signalling Leading to an Impaired Cytotoxic Response.” *Leukemia* 27 (3): 650–60. https://doi.org/10.1038/leu.2012.285.

Silver, Nicholas, Steve Best, Jie Jiang, and Swee Lay Thein. 2006. “Selection of Housekeeping Genes for Gene Expression Studies in Human Reticulocytes Using Real-Time PCR.” *BMC Molecular Biology 2006 7:1* 7 (1): 1–9. https://doi.org/10.1186/1471-2199-7-33.

Sotthibundhu, Areechun, Katya McDonagh, Alexander von Kriegsheim, Amaya Garcia-Munoz, Agnieszka Klawiter, Kerry Thompson, Kapil Dev Chauhan, et al. 2016. “Rapamycin Regulates Autophagy and Cell Adhesion in Induced Pluripotent Stem Cells.” *Stem Cell Research & Therapy* 7 (1): 1–16. https://doi.org/10.1186/S13287-016-0425-X.

Taira, Takaomi, Tomonori Kobayashi, and Tomokatsu Hori. 2003. “Disappearance of Self-Mutilating Behavior in a Patient with Lesch-Nyhan Syndrome after Bilateral Chronic Stimulation of the Globus Pallidus Internus: Case Report.” *Journal of Neurosurgery* 98 (2):

414–16. https://doi.org/10.3171/jns.2003.98.2.0414.

Takahashi, Kazutoshi, Koji Tanabe, Mari Ohnuki, Megumi Narita, Tomoko Ichisaka, Kiichiro Tomoda, and Shinya Yamanaka. 2007. "Induction of Pluripotent Stem Cells from Adult Human Fibroblasts by Defined Factors." *Cell* 131 (5): 861–72. https://doi.org/10.1016/j.cell.2007.11.019.

Thomas, Kirk R., and Mario R. Capecchi. 1987. "Site-Directed Mutagenesis by Gene Targeting in Mouse Embryo-Derived Stem Cells." *Cell* 51 (3): 503–12. https://doi.org/10.1016/0092-8674(87)90646-5.

Torres, R. J., C. Prior, and J. G. Puig. 2006. "Efficacy and Safety of Allopurinol in Patients with the Lesch-Nyhan Syndrome and Partial Hypoxanthine- Phosphoribosyltransferase Deficiency: A Follow-up Study of 18 Spanish Patients." *Https://Doi.Org/10.1080/15257770600893974* 25 (9–11): 1077–82. https://doi.org/10.1080/15257770600893974.

Torres, Rosa J., and Juan G. Puig. 2007. "Hypoxanthine-Guanine Phosophoribosyltransferase (HPRT) Deficiency: Lesch-Nyhan Syndrome." *Orphanet Journal of Rare Diseases*. BioMed Central. https://doi.org/10.1186/1750-1172-2-48.

Villa, Elodie, Eunus S. Ali, Umakant Sahu, and Issam Ben-Sahra. 2019. "Cancer Cells Tune the Signaling Pathways to Empower de Novo Synthesis of Nucleotides." *Cancers* 11 (5). https://doi.org/10.3390/CANCERS11050688.

Visser, Jasper E, Adam C Cotton, David J Schretlen, Jocelyne Bloch, Kristina Tedroff, Gastón Schechtmann, Diana Radu Djurfeldt, Victoria Gonzalez, Laura Cif, and Hyder A Jinnah. 2021. "Deep Brain Stimulation in Lesch–Nyhan Disease: Outcomes from the Patient's Perspective." *Developmental Medicine & Child Neurology* 63 (8): 963–68.

https://doi.org/10.1111/DMCN.14852.

Watts, R. W.E., E. Spellacy, D. A. Gibbs, J. Allsop, R. O. McKeran, and G. E. Slavin. 1982. "Clinical, Post-Mortem, Biochemical and Therapeutic Observations on the Lesch-Nyhan Syndrome with Particular Reference to the Neurological Manifestations." *QJM: An International Journal of Medicine* 51 (201): 43–78. https://doi.org/10.1093/oxfordjournals.qjmed.a067707.

Yeh, Jason, Shuang Zheng, and Bruce D. Howard. 1998. "Impaired Differentiation of HPRT-deficient Dopaminergic Neurons: A Possible Mechanism Underlying Neuronal Dysfunction in Lesch-Nyhan Syndrome." *Journal of Neuroscience Research* 53 (1): 78–85. https://doi.org/10.1002/(SICI)1097-4547(19980701)53:1<78::AID-JNR8>3.0.CO;2-G.

Yin, Jie, Wenkai Ren, Xingguo Huang, Jinping Deng, Tiejun Li, and Yulong Yin. 2018. "Potential Mechanisms Connecting Purine Metabolism and Cancer Therapy." *Frontiers in Immunology* 0 (July): 1697. https://doi.org/10.3389/FIMMU.2018.01697.

Zaccolo, Manuela. 2011. "Spatial Control of CAMP Signalling in Health and Disease." *Current Opinion in Pharmacology* 11 (6): 649–55. https://doi.org/10.1016/J.COPH.2011.09.014.

Appendices

Copyright Permission

The manuscript on which this thesis is based was published under a creative commons license in Stem Cell Reports by Cell Press.

Included in the Author's Rights list published by Cell Press is the right to: "Include the article in full or in part in a thesis or dissertation (provided that this is not to be published commercially)."

For more information: https://www.cell.com/trends/editorial-policies

Research Ethics Approval (Renewed 2021)

Centre intégré universitaire de santé et de services sociaux de l'Ouest-de-l'Île-de-Montréal
Québec

Comité d'éthique de la recherche de l'Institut universitaire en santé mentale Douglas

BY ELECTRONIC MAIL

February 19, 2021

Carl Ernst, PhD
Principal Investigator
Assistant Professor
Department of Psychiatry
McGill University

RE: Annual Renewal of the research ethics approval for "INVESTICATE: Identification of New Variation, Establishment of Stem cells, and Tissue Collection Aimed at Treatment Efforts"
IUSMD-15-14
Funding agency: McGill University

Dear Dr. Ernst,

The Research Ethics Board (REB) of the Douglas Mental Health University Institute, which acts as the evaluating REB for the above-mentioned research project, received on February 9, 2021 the documents that you have submitted for the annual renewal of ethics approval. The documents are as follows:

- INVESTICATE-renew-2021-signed

It has been determined that the review of your documents could be delegated in accordance with section 6.12 of the *Tri-Council Policy Statement* (TCPS 2) as there is no information to suggest that the level of risk could have changed. We are happy to inform you that on February 18, 2021, the REB Chair or a delegate reviewed your documents, and has re-approved the project.

The ethical approval of your project is therefore renewed for a period of one year, from March 14, 2021 to March 14, 2022. The members of the REB will be informed of this decision at the following full board meeting and the decision will be noted in the minutes.

During this renewed approval period, you agree to:

- Submit any new letter of authorization from persons formally mandated to authorize the carrying out of research projects or any modification to pre-existing authorizations
- Submit an amendment if you wish to make a change to the consent forms or protocol such as, for example, adding a researcher to the project, changing the recruitment methods, increasing the number of participants, using a new questionnaire, or changing the analysis plan;
- Submit an annual report duly completed and signed no later than 30 days before the end of the renewal period if you wish to continue the project beyond this period;
- Submit a completed and signed end of study report when all research activities are completed;

6875, boulevard LaSalle, FBC 1116
Montréal (Québec) H4H 1R3
Téléphone : 514 761-6131 poste 2708
www.ciusss-ouestmtl.gouv.qc.ca

- Submit an incident or deviation report if such a situation occurs.

Annual reports for renewals and end of study reports should be submitted to recherche.comtl@ssss.gouv.qc.ca. Amendment forms, acknowledgment requests, incident reports and deviation reports should be submitted to cer.reb@douglas.mcgill.ca. All documents can be downloaded from https://douglas.research.mcgill.ca/en/suivi-continu

For any questions regarding this decision or your research project, please contact the REB office by phone at 514-761-6131, extension 2708 or by email at cer.reb@douglas.mcgill.ca.

Thank you for your attention to this matter,

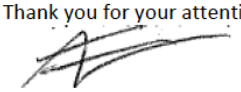

Fredrick Vokey, MA
Planning, Programming and Research Officer – research ethics
University Affairs, Teaching and Research Directorate
Montréal West Island Integrated University Health and Social Services Centre

On behalf of:
Joseph Rochford, PhD
Chair, Research Ethics Board
Douglas Mental Health University Institute

cc: Research Ethics Board of the Douglas Mental Health University Institute